applied sciences

MDPI

Article

A New Method of Investigation of the Orientation of Galaxies in Clusters in the Absence of Information on Their Morphological Types

Włodzimierz Godłowski *,† **and Błażej Mrzygłód** †

Institute of Physics, Uniwersytet Opolski, ul. Oleska 48, 45-052 Opole, Poland; blazmrzy@interia.eu
* Correspondence: godlowski@uni.opole.pl
† These authors contributed equally to this work.

Abstract: The analysis of the orientation of galaxies is one of the most widely used tools in the fields of extragalactic astronomy and cosmology, enabling the verification of structure formation scenarios in the universe. It is based on the statistical analysis of the distribution of angles, giving the spatial orientation of galaxies in space. In order to obtain the correct analysis results, one is obliged to take into account the Holmberg effect and the fact that galaxies are oblate spheroids, with the real axis ratio depending on the morphological type. However, most of the astronomical data available today do not contain information about the morphological types of galaxies. The analysis of sufficiently numerous observational data allows one to calculate the estimated frequency of the occurrence of given morphological types used in the proposed method. As a part of this, on the basis of these frequencies, simulations were performed, which enabled us to recognize new angle distributions used in orientation studies. These distributions already contain information on the frequency of the appearance of galaxies of particular morphological types in clusters, allowing for more accurate results of the statistical tests carried out during the analysis. The method is an extension of results developed in in our previous investigations.

Keywords: orientation of galaxies; galaxies clusters; morphological types of galaxies

check for updates

Citation: Godłowski, W.; Mrzygłód, B. A New Method of Investigation of the Orientation of Galaxies in Clusters in the Absence of Information on Their Morphological Types. *Appl. Sci.* **2023**, *13*, 4845. https://doi.org/10.3390/app13084845

Academic Editor: Marios Chatzikos

Received: 28 February 2023
Revised: 8 April 2023
Accepted: 9 April 2023
Published: 12 April 2023

Copyright: © 2023 by the authors. Licensee MDPI, Basel, Switzerland. This article is an open access article distributed under the terms and conditions of the Creative Commons Attribution (CC BY) license (https://creativecommons.org/licenses/by/4.0/).

1. Introduction

The current state of knowledge about galaxies, their clusters and the universe itself has made significant progress. There exist various theoretical models describing galaxy formation and their structures, each with different predictions on galaxy orientations in structures, distributions of galactic angular momentum, and collinearity between the location of the brightest galaxy and the major axis of the structure. To verify these expectations and the validity of a particular model, observations are compared with theoretical predictions. This means that the study of galaxy angular momentum distributions is a simple but very important test for the correctness of various models of galaxy formation and their structures [1–3].

In the commonly accepted ΛCDM cosmological model, one considers the universe to be spatially flat, isotropic and homogeneous in an appropriately large scale. According to the model, structures are formed from primordial, adiabatic, self-scaling Gaussian fluctuations [4–7]. These assumptions underpin the hierarchical clustering model. Variants that take into account non-Gaussian initial fluctuations are also successfully developed [7]. The analysis of galaxies and their clusters should provide evidence confirming the postulated origins of structures in the universe, and one of such forms is the study of the orientation of galaxies. These analyses assume that normals to the galaxies' planes are their rotation axes, which is especially true for spiral galaxies. The analysis of the distribution position angles of the galaxy major axes, as well as two angles describing the spatial orientation of the galaxy plane, give information about the orientation of galaxies in space and galaxy

angular momenta. The investigations described provide a standard method for testing models of galaxy formation because these models predict different outcomes regarding the orientation of galaxies within structures, the distribution of galactic spins, and the alignment between the brightest galaxy and the major axis of the structure [3,8–14].

It is not too difficult to analyze the orientation of galaxies in space, and as a result, the distribution of the angular momenta for the luminous matter. Unfortunately in the real universe, luminous galaxies and their structures are surrounded by dark matter halos. These halos are often much more extended and massive than the luminous component of the structures. Unfortunately, dark matter is invisible, and as an result, the direct observation of dark matter halos and their angular momentum is much more complicated. However, as we obBy observing the correlations between luminous and dark matter (sub)structures, we can conclude that there is a dependence between dark matter halos and luminous matter (real galaxies) in terms of the direction of the angular momentum (see for example [15,16]). The results of Okabe et al. (2018) and Codis et al. (2018) [17,18], based on Horizon-AGN simulations, also show a similar dependence. This allowed for a conclusion that the analysis of angular momentum of luminous matter gives us information about the angular momentum of the total structure as well. As result, the analysis of the angular momentum of "real" (luminous) galaxies and their structures is still important as a test of structure formation.

The problem of analyzing the alignment of galaxies with different structural scales is very important. This problem, as well as the alignment of galaxies in the larger group, was analyzed many times, both theoretically (see for example [19,20]) and observationally, for example, by Thompson (1976) [21]. The most significant finding is that there is no conclusive evidence supporting the alignment of galaxies in groups and poor clusters of galaxies, whereas ample evidence exists for rich clusters of galaxies. Furthermore, the alignment of galaxies increases with the richness of the structures [7,9,22].

Alignment in the large-scale has also been studied many times, starting with the work of Hutsemekers [23], Hutsemeker's research group analyzed the polarization vectors of quasars. Based on a new sample of 355 quasars with significant optical polarization, they found that the polarization vectors of the quasars are not randomly oriented on the celestial sphere [24]. The polarization vectors show an order on a scale of about 1 Gpc. In addition, the average polarization angle rotates with redshift, by about 30° per Gpc. Anisotropy in cosmology was later confirmed by many authors—see, for the most recent review, [25].

Two main methods of studying the orientation of galaxies have crystallized over the years. The authors of the first of them are Hawley and Peebles [26], who in their approach used the statistical analysis of the distributions of galaxy position angles in order to detect possible deviations from the isotropic distribution. As part of the approach, the χ^2, First Autocorrelation and Fourier tests were introduced, which have become a standard method in this type of research [21,22,27]. This approach has a flaw, however, in that position angles only give good information about the orientations of galaxy planes for side-viewed galaxies.

An alternative method was originally proposed by Öpik [28], applied by Jaaniste and Sarr [29,30], and significantly modified by Flin and Godłowski [9,31]. It uses not only the position angles of galaxies, but also their ellipticities, making it possible to include galaxies with all possible settings and positions on the celestial sphere in the study. Obtaining correct results, however, obliges one to take into account the Holmberg effect in the analysis, which consists of the fact that the measured, especially optical, ellipticity of the image of galaxies differs from the true ellipticity of the image [32–35], and the fact that galaxies are flattened spheroids with the actual axis ratio depending on their morphological type.

The method of analysis of the alignment of galaxies in clusters originally proposed in the papers Godłowski (2012) and Pajowska et al. (2019) [9,27] has been greatly improved. The analysis of the spatial orientation of the galaxies from deprojection of their images required, in classical form, knowledge of morphological types of galaxies, which is rare with modern Kilo-Degree Surveys. Unfortunately, most of the currently available astronomical data do not provide information on the morphological types of galaxies. For this

reason, research works, e.g., by Tully [36], use the averaged values of the real ratio of the galaxies' axes. This solution may be insufficient in some cases, therefore, an alternative method is proposed [9,37–40], consisting of estimating the fraction of galaxies of a given morphological type. A new version of the method used for analyzing the orientation of galaxies in clusters, presented in the current work, makes it possible to carry out such an analysis, also in the case of the absence of information on their morphological types. We present the practical applications of this new variant of our method, as well as the implications of the results with reference to theories of galaxy formation.

2. Observational Data

Because our method is new, we decided to test it on a well-known and tested sample of galaxies and their structures, in order to free ourselves from not fully controlled observational and systematic effects. As part of the implementation of the method, the Tully Nearby Galaxies (NBG) Catalog [36] was used. This catalog was chosen because it contains all the necessary information about both individual galaxies and their structures. In particular, it has been carefully screened for the completeness of the sample and the removal of non-galactic objects from it. One should note that the NBG Catalog is complete up to the magnitude limit $B_T^{b,i} = 12.0$ [41]. Additionally, it includes dimmer, low-surface brightness gas-rich galaxies (late-type spirals), ensuring that all more massive galaxies are taken into account. Due to the position of the Galaxy with respect to the center of the Local Supercluster (LSC), which is the Virgo Cluster, it is complete for such objects only up to the Virgo Cluster center. The Catalog contains 2367 galaxies with radial velocities (corrected to the motion of the Sun) lower than 3000 $\frac{\text{km}}{\text{s}}$ and devoid of background objects. The Tully Catalog provides relatively even coverage of the entire unobstructed sky [41]. Position angles not included in the catalog were taken from [42–45], and missing measurements were made on Palomar Sky Survey prints by Flin [8]. For face-on galaxies, for which it was impossible to determine the position angles, their random distribution was assumed (for face-on galaxies, the value of the position angles has a minimal effect on the orientation of the galaxy space—see the next chapter). The catalog contains information on the morphological types of galaxies, therefore, it enables qualitative verification of the effectiveness of the proposed method. The NBG catalog also lists galaxy group and subgroup affiliations for all galaxies in the catalog. Groups were selected in a uniform way based on angular and distance separation. Tully selected 366 groups of two or more members involving 1525 galaxies (64% of all NBG galaxies) [41]. The distances of galaxies are determined by velocity, assuming the Einstein de Sitter model or the flat dust model with the deceleration parameters $q_0 = 1/2$ (for historical reasons, q_0 denotes the deceleration parameter in this case) and $H_0 = 75\text{km s}^{-1}\text{Mpc}^{-1}$, as well as the velocity perturbation model near the Virgo Cluster [46]. The use of the simpler Einstein de Sitter model instead of ΛCDM is justified, because the range of the NBG catalog [36] is $z = 0.01$, and up to distances corresponding to $z = 0.2$, the differences between the distances calculated in different cosmological models are minimal. This means that the distances of the galaxies are determined in a very good and homogeneous way. As a result, lists of galaxies included in particular galaxy groups are free from foreground and background objects, which is essential when analyzing small numbers of galaxy structures. In our opinion, the groups selected according to the precise criteria in the Tully catalog are an example of one of the best group selections. The use of the catalog in other research works [8,47–49] also makes it possible to indicate the correlation of the obtained results. In the present work, during the implementation of the method, only those groups from the NBG Catalog that have at least 40 members are used. There are 18 such groups.

3. Method of the Investigation

The proposed new method for investigating the orientation of galaxies in clusters is an extension of the approach presented in [9,22,27,31,48,49]. According to the method developed by Flin and Godłowski [31], and by Godłowski [9,22], one calculates the "polar"

angle δ_D, which is the angle between the normal to the galaxy plane and the main plane of the coordinate system, and the "azimuth" angle η, describing the direction between the projection of this normal onto the main plane and the direction towards the zero initial meridian. Using a supergalactic coordinate system (in this case, the main plane is supergalactic equator), these angles can be expressed as the relationship between the latitude and longitude angles, B and L, the position angle P, and the inclination angle i (Figure 1). Since galaxies are oblate spheroids [32], determining a galaxy's angular return using only its image is problematic, all the more so as the galaxy can be aligned in relation to the observer in four ways, giving the same number of possible rotation axes, as it is easily seen in Figure 1. If (as in our case) we do not have data on the rotational direction of the galaxies, it is sufficient to study only the line segment directed normal to the galaxy planes inside the sphere. This implies the need to consider only two possible orientations of galaxies. As a result, the formulas for calculating the angles δ_D and η take the form:

$$\sin \delta_D = -\cos i \sin B \pm \sin i \cos r \cos B, \tag{1}$$

$$\sin \eta = (\cos \delta_D)^{-1}[-\cos i \cos B \sin L + \sin i(\mp \cos r \sin B \sin L \pm \sin r \cos L)], \tag{2}$$

$$\cos \eta = (\cos \delta_D)^{-1}[-\cos i \cos B \cos L + \sin i(\mp \cos r \sin B \cos L \mp \sin r \sin L)], \tag{3}$$

$$S = -\cos i \cos B \mp \sin i \cos r \sin B, \tag{4}$$

$$r = P - \frac{\pi}{2}. \tag{5}$$

Obtaining a random distribution obliges us to change the sign of the δ_D angle to the opposite one for any value of parameter S that is smaller than zero [22,31]. Please note, that for face-on galaxies, the inclination angle i is close to 0. As a result, $\sin i$ is also close to zero, and the position angle has a minimal effect on the spatial orientations of the face-on galaxies.

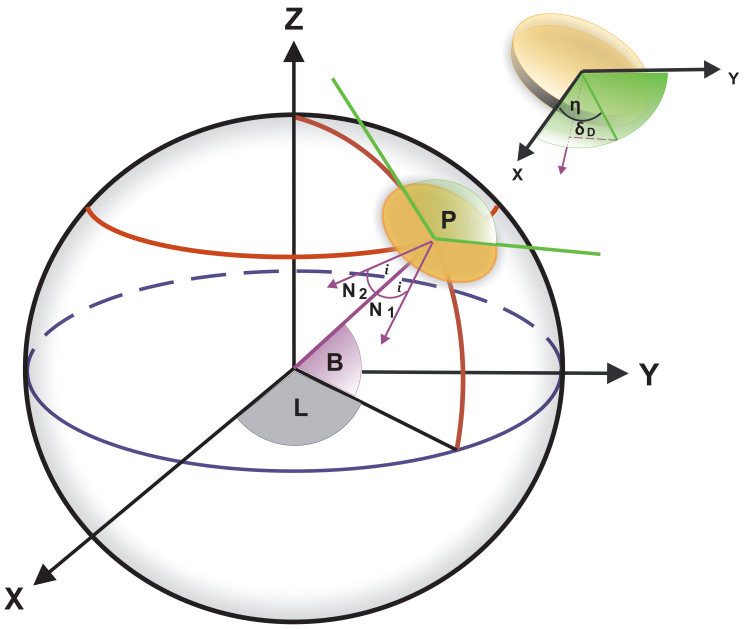


Figure 1. A schematic illustration of angles δ_D (the polar angle between the normal to the galaxy plane and the main plane of the coordinate system) and η (the azimuth angle between the projection of this normal onto the main plane and the direction towards the zero initial meridian). The angle of inclination i is the angle between the normal to the plane of the galaxy observer's line of sight, while P is the angle of the position in the frame of reference. N_1 and N_2 are possible positions of the normal to the galaxy plane-directed line segment inside the sphere. If we were also interested in the rotation

direction of the galaxy, we would have two more normal vectors, N_1' and N_2', which are different from vectors N_1 and N_2 in that they would be comprise a directed line segment outside the sphere. L and B are the longitude and latitude of the reference coordinate system (for more details see Pajowska [9], Godłowski [31], Aryal et al. [50]).

Any statistical study involving orientations must take into account the fact that directional variables are cyclic [51], and moreover, in theory, the "random" distribution of analyzed angles can be not uniform. As a result, tests statistics could be significantly modified and must be obtained from simulations (see [9] for detailed discussion) or from tests specially dedicated to this problem, such as the Cramer-von Mises test [52,53] and Watson test [54,55].

The value of the inclination angle can be obtained using the Holmberg formula, which is valid for oblate spheroids [32]

$$i = \cos^{-1}\left(\sqrt{\frac{q^2 - q_0^2}{1 - q_0^2}}\right), \tag{6}$$

$q = \frac{d}{D}$ is the ratio of the minor to the major axis diameters, and q_0 is the "true" axial ratio. Using the Heidmann, Heidmann and de Vaucouleurs (HHD) approach [56], each morphological type can be assigned a corresponding value for the parameter q_0.

A different approach was taken by Tully in his catalog [36], using an averaged q_0 of 0.2. This averaged value had previously appeared in Holmberg 's paper [32]. To compensate for not taking into account the different morphological types of galaxies, Tully added a 3° contribution to the calculated inclination angles

$$i = \cos^{-1}\left(\sqrt{\frac{q^2 - 0.2^2}{1 - 0.2^2}}\right) + 3^\circ. \tag{7}$$

3.1. Statistical Methods

Because in the investigation we have an uniform distribution of angles the sphere, numerous ranges of the polar δ_D and azimuthal η angles should be characterized by successively cosine and uniform distributions. The analysis of these distributions is possible with the use of statistical methods, proposed for the first time in the paper of Hawley and Peebles: the χ^2 test, the First Autocorrelation test and the Fourier test, and additionally the Kolmogorov–Smirnov test, Cramer-von Mises test and Watson test . Within them, the tested range of the test angle θ is divided into n, equal to the width of bins. In the conducted research, the range of the test angle was divided into 18 bins. The test angle is equal, in this case, to $\delta_D + \frac{\pi}{2}$ or η. The obtained real numbers of galaxies in the k-th bin N_k are confronted with the theoretical numbers of galaxies $N_{0,k}$ in these bins.

The χ^2 test uses the statistic:

$$\chi^2 = \sum_{k=1}^{n} \frac{(N_k - Np_k)^2}{Np_k} = \sum_{k=1}^{n} \frac{(N_k - N_{0,k})^2}{N_{0,k}} \tag{8}$$

where N is the total number of galaxies in the cluster under consideration, and p_k is the probability that the selected galaxy will fall into the k-th range. For n intervals, the number of degrees of freedom of the χ^2 test is $n - 1$, therefore, the expected value is $E(\chi^2) = n - 1$, and the variance is expected to be $\sigma^2(\chi^2) = 2(n - 1)$. For 18 bins, the expected value is $E(\chi^2) = 17$ with variance $\sigma(\chi^2) = 5.831$. For the assumed confidence level of $\alpha = 0.05$, the critical value of the test is $\chi^2_{cr} = 27.587$.

It should be noted, however, that the statistic described by the above equation has only limited χ^2 distribution. As a result, in the case of real analysis, the distribution of our statistic given by Equation (8) may be different than that described by the theoretical distribution χ^2 [57–59], and should be obtained from numerical simulations. The correct-

ness of the approximation of the distribution of our statistics by χ^2 distributions in galaxy orientation studies was analyzed in Pajowska et al., 2019 [9].

A different approach is presented by the First Autocorrelation test [26]. It should be noted here that the standard and probably the best test of autocorrelation is the von-Neumann–Durbin–Watson test. However, in our article, we do not use full autocorrelation, and although the test limited to the First Autocorrelation test may not perform as well as the von-Neumann–Durbin–Watson test, the idea presented there is also widely used (see, for example, Percival & Walden [60]—especially chapter 6 of the book). So, it seems that the use of this test works well enough. The usefulness and correctness of using the First Autocorrelation test in research in terms of ordering the orientation of galaxies has been shown in the work of Pajowska et al., 2019 [9].

The First Autocorrelation test determines the correlations between galaxy numbers in neighboring angle bins, which is given by the statistic:

$$C = \sum_{k=1}^{n} \frac{(N_k - N_{0,k})(N_{k+1} - N_{0,k+1})}{[N_{0,k} N_{0,k+1}]^{\frac{1}{2}}} \tag{9}$$

where $N_{n+1} = N_1$. In the paper of Hawley and Peebles [26], it was calculated that the expected value $E(C) = 0$, while the standard deviation $\sigma(C) = \sqrt{n}$. According to the paper of Godłowski [27], it was shown that this result is only an approximation for the case in which all $N_{0,k}$ are equal, with the expected value $E(C) = -1$. The correct value of the variance of the C statistic is only approximately equal to n, and must be obtained from numerical simulations.

The Fourier test originally appeared in the paper of Hawley and Peebles [26]. However, only the first two modes were analyzed at that time. This test was significantly improved by Godłowski [27], in which higher Fourier modes are taken into account. In the Fourier test, deviation from isotropy is a slowly varying function of the angle θ, according to the relationship:

$$N_k = N_{0,k}(1 + \Delta_{11} \cos 2\theta_k + \Delta_{21} \sin 2\theta_k + \Delta_{12} \cos 4\theta_k + \Delta_{22} \sin 4\theta_k + \ldots) \tag{10}$$

In this case, all $N_{0,k}$ are equal. The Fourier coefficients are given by the following formulas:

$$\Delta_{1J} = \frac{\sum_{k=1}^{n} (N_k - N_{0,k}) \cos 2J\theta_k}{\sum_{k=1}^{n} N_{0,k} \cos^2 2J\theta_k} \tag{11}$$

$$\Delta_{2J} = \frac{\sum_{k=1}^{n} (N_k - N_{0,k}) \sin 2J\theta_k}{\sum_{k=1}^{n} N_{0,k} \sin^2 2J\theta_k} \tag{12}$$

with standard deviations given by:

$$\sigma(\Delta_{1J}) = \left(\sum_{k=1}^{n} N_{0,k} \cos^2 2J\theta_k \right)^{-\frac{1}{2}} \tag{13}$$

$$\sigma(\Delta_{2J}) = \left(\sum_{k=1}^{n} N_{0,k} \sin^2 2J\theta_k \right)^{-\frac{1}{2}} \tag{14}$$

Analysis using the Fourier test allows us to determine the direction of departure from isotropy. For negative values of the coefficient Δ_{11}, there is a predominance of galaxies with the position angle parallel to the Local Supercluster plane. For positive values of this coefficient, there is a predominance of galaxies with the position angle being perpendicular to the Local Supercluster plane. When analyzing the angle η, negative values of the coefficient Δ_{11} indicate a predominance of galaxies with η perpendicular to the 0 meridian coordinate system, while positive values of this coefficient indicate a predominance of galaxies with η pointed parallel to the 0 meridian. However, when investigating the δ_D

angles, negative values of the coefficient Δ_{11} indicate a predominance of galaxies with normals parallel to the main plane of the coordinate system, while positive values of this coefficient indicate a predominance of normals perpendicular to the main plane.

The probability that the amplitude

$$\Delta_J = \left(\Delta_{1J}^2 + \Delta_{2J}^2\right)^{-\frac{1}{2}} \tag{15}$$

described by the two-dimensional Gaussian distribution, is greater than a certain chosen value is given by the formula:

$$P(>\Delta_J) = \exp\left(-\frac{1}{2}\left(\frac{\Delta_{1J}^2}{\sigma(\Delta_{1J}^2)} + \frac{\Delta_{2J}^2}{\sigma(\Delta_{2J}^2)}\right)\right). \tag{16}$$

By using the auxiliary variable $J = \Sigma_i \Sigma_j G_{ij} I_i I_j$, where G is the inverse matrix to the covariance matrix of Δ_{ij}, it is possible to write:

$$P(>\Delta_1) = \exp\left(-\frac{1}{2}J\right), \tag{17}$$

where the vector $\mathbf{I}$ is:

$$\mathbf{I} = \begin{pmatrix} \Delta_{11} \\ \Delta_{21} \end{pmatrix}. \tag{18}$$

The probability that the amplitude

$$\Delta = \left(\Delta_{11}^2 + \Delta_{21}^2 + \Delta_{12}^2 + \Delta_{22}^2\right)^{-\frac{1}{2}} \tag{19}$$

described by the four-dimensional Gaussian distribution, is greater than a certain chosen value is given by the formula:

$$P(>\Delta) = \left(1 + \frac{1}{2}J\right)\exp\left(-\frac{1}{2}J\right), \tag{20}$$

where vector $\mathbf{I}$ has the form:

$$\mathbf{I} = \begin{pmatrix} \Delta_{11} \\ \Delta_{21} \\ \Delta_{12} \\ \Delta_{22} \end{pmatrix} \tag{21}$$

(a detailed discussion of the Fourier test is included in Appendix A).

It should be mentioned here that, against the use of the Fourier test [26], it has been argued that, from a theoretical point of view, the application of the Fourier transform does not lead to the correct result, because the conditions under which we get exponential probability formulas (Equation (16)) rarely work in practice (see [60], Chapter 5). This problem is well-known and discussed many times in the literature in the context of the utility of power spectrum analysis (PSA) [61–63]. Newman et al. (1994) [62] pointed out that Yu & Peebles (1969) showed that the Power Spectrum Analysis version [61] only applies exactly when the uniform distribution function is tested. In other cases, test statistics are modified [60,62] and must be simulated (see also [63]). The correctness and usefulness of using the Fourier test in the alignment of galaxy studies were analyzed in the paper by Pajowska et al., 2019 [9], where it was found that in the case of the analysis of position angles it works perfectly well. Moreover, because formulae for Δ_i are obtained by maximum-likelihood methods, they have limited normal distributions. As a result, even for angles δ_d giving the spatial orientation, this approximation works well enough.

In the Kolmogorov–Smirnov test, the D_n statistic is calculated,

$$D_n = \sup |F(x) - S(x)| \tag{22}$$

which is the largest absolute difference between the theoretical distribution function $F(x)$ and the empirical distribution function $S(x)$, calculated on the basis of an ordered sample (sup in Equation (22) denotes the supremum). It is assumed that the theoretical, random distribution contains the same number of objects as the observed one. The value of the obtained statistics

$$\lambda = \sqrt{n} D_n \tag{23}$$

should be lower than the critical value λ_{cr} obtained for a given confidence level α, in accordance with the Smirnow formula [64]. For the assumed confidence level of $\alpha = 0.05$, the critical value $\lambda_{cr} = 1.358$.

In the Cramer von-Mises test [52,53], the W^2 statistic is computed:

$$W^2 = \sum_{i=1}^{n} \left(F(x_i) - \frac{2i-1}{2n} \right)^2 + \frac{1}{12n} \tag{24}$$

where $F(x_i)$ is again the theoretical distribution. In the advanced modification, called the Watson test [54,55], one uses the statistic:

$$U^2 = W^2 - n \left(\bar{F} - \frac{1}{2} \right)^2 \tag{25}$$

where the average value $\bar{F} = \frac{1}{n} \sum_{i=1}^{n} F(x_i)$.

As we noted above, for some tests, it is difficult to obtain the critical value theoretically, and in practical applications, it must be obtained from simulations. For that, we obtained the Cumulative Distribution Function (CDF) from 1000 simulations. At first, we compared CDF obtained for four Tully cluster (detailed see in Section 4) in the case χ^2 test . Because CDF was very similar, it was enough to run these simulations for just one cluster. In the Figure 2, the CDF values for the statistic χ^2, First Autocorrelation test and Fourier test are presented (angle δ_D on left panel while angle η on right panel). For the Kolmogorov, Cramer von-Mises and Watson tests, where binning process is crucial (see [9]), the CDF is presented in the Appendix B. From Figures 2 and A1 it is easy to find the critical value of statistics at different confidence levels.

3.2. Assumptions of a New Method of Investigation

According to the new approach used in the proposed method, the investigation of the orientation of galaxies in clusters, in the absence of information on the morphological types of each galaxy separately, can be carried out, taking into account the estimated frequencies of occurrence of given morphological types [9,37–40]. A calculation of these frequency estimates is possible by analyzing a sufficiently large number of observational data. In our work, fortunately, we have information about the morphological types of all galaxies in clusters, so we could use the frequency of occurrence of individual morphologies in the same way as we would when using real data. Assuming an isotropic distribution of normals to the plane of the galaxy in space, we generate an isotropic random distribution of inclination angles. By using the known frequencies of occurrence of given morphological types and the HHD approach for parameter q_0, we can reverse the Formula (6) and obtain a new "isotropic" distribution of the "observed" axial ratio q. This allows us to perform numerical simulations for the examined clusters of galaxies, which enable us to learn new values of the angle i through Formula (7) or any other similar formula. Using these new values of i, we can then calculate new values of angles δ_D and η. "Theoretical isotropic distributions" of angles δ_D and η contain information about the frequency of appearance of galaxies of particular morphological types in clusters. For analyzing the transition to

δ_D and η, we need to set the locations of the galaxies in space. Because we analyzed the orientations of galaxies in specific groups, we took the exact coordinates of real galaxies. Only the use of these new distributions makes it possible to test the isotropy hypothesis of the orientation of galaxies in the case of unknown morphological types.

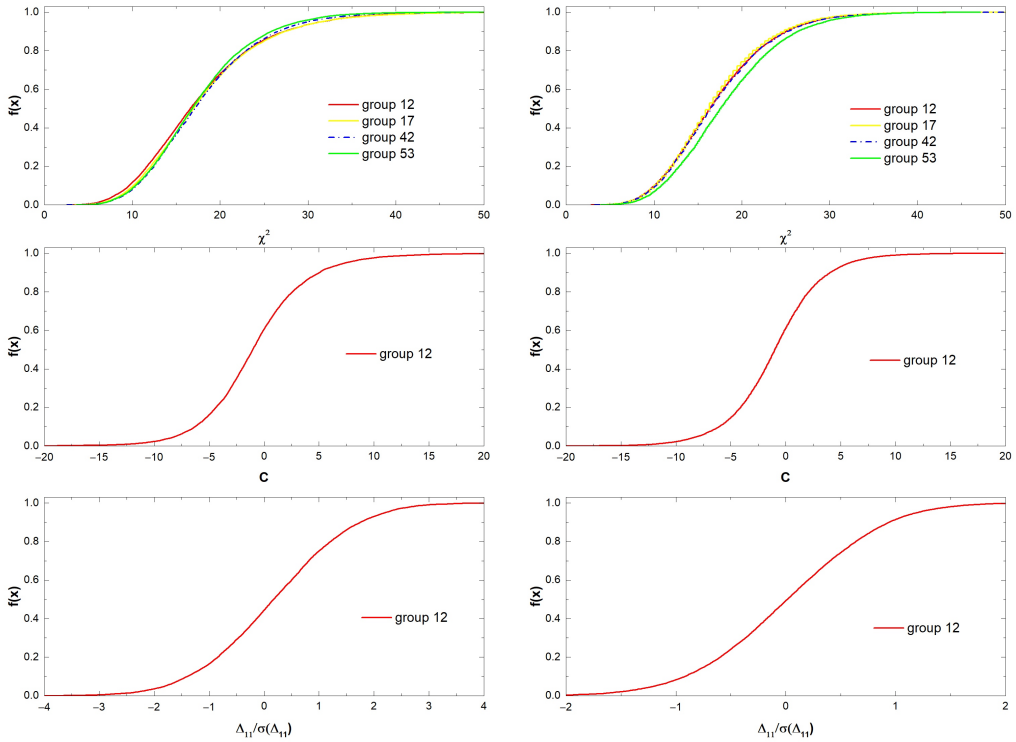


Figure 2. The Cumulative Distribution Function (CDF) of the angle δ_D (left panel) and η (right panel) for analyzed statistics. From up to down are presented statistics: χ^2, C and $\frac{\Delta_{11}}{\sigma(\Delta_{11})}$.

4. The Results

Data from the Tully Catalog were subjected to some statistical tests, among others in [48,49]. Tables 1 and 2 present an analysis of the orientation of galaxies in the Tully groups, using inclination angles taken directly from the NBG Catalog to obtain angles δ_D and η, where statistically significant results showing strong anisotropy were marked in a bold font. The obtained results show a non-randomness of the distribution of the δ_D angle for groups 11, 31, 41, 51 and 52, and in the case of the η angle for groups 11, 12, 31, 41, 51, 52 and 64. In the paper of Godłowski [48] it was shown that for all groups, there should be a random distribution of angles, giving the spatial orientation of the galaxies. For this purpose, the study should take into account the morphological types of galaxies [56], and convert q to the standard photometrical axial ratios according to Fouque and Paturel (FP) formulae [35]. Our main goal is to introduce a new method of studying the orientation of galaxies in clusters, when we do not know the morphological type of individual galaxies. We also wanted to investigate whether this effect alone could explain the observed ordering of galaxies in Tully's clusters. It is for this reason that we started our research by simulating the impact of this effect, and added the FP photometric correction (as well known for galaxies from the NBG Tully catalog) at the end. Tables 3 and 4 show the analysis of the orientation of galaxies using inclination angles, based on the morphological type of galaxies (taken from the NBG catalog), but without Fouque and Paturel correction. It turns out that in the case of the Tully Catalog, just taking into account the morphological types of galaxies is not enough to get the isotropic distribution. We expect such a distribution because of theoretical predictions that the alignment of galaxies increases with structural mass, while observational studies show that there are no satisfactory evidence for the alignment of galaxies in groups and poor clusters of galaxies. In the case of the results presented in

Tables 3 and 4, it should be emphasized that the mere calculation of the inclination angles on the basis of the q axial ratio values contained in the catalog changes the values of the obtained statistical tests. This is due to the different origins of the inclination angles included in the catalog, some of which have been calculated according to the Tully (7) formula. This is visible when all inclination angles are calculated in accordance with the Tully (7) formula, and is represented by the values of statistical tests presented in Tables 5 and 6. The comparison of Tables 1–6 shows the noticeable influence of the method of determining the value of the inclination angle on the value of the statistical tests obtained.

Table 1. Test for the isotropy of the orientations of the galaxy plane. The distribution of the angle δ_D of galaxies; inclination was taken directly from the NBG Catalog.

Group	N	χ^2	C	$P(\Delta_1)$	$P(\Delta)$	Δ_{11}	$\sigma(\Delta_{11})$	$\frac{\Delta_{11}}{\sigma(\Delta_{11})}$	λ	W^2	U^2
11	626	**62.79**	**9.505**	**0.0002**	**0.0004**	−0.2365	0.0585	−4.0459	1.197	0.6769	−0.1641
12	332	25.67	−11.484	0.2992	0.6338	−0.1247	0.0803	−1.5534	0.549	0.1183	−0.3470
13	128	29.72	−6.939	0.9148	0.9438	0.0022	0.1293	0.0174	0.621	0.0726	−0.0905
14	426	23.96	3.524	0.1700	0.2538	−0.1201	0.0709	−1.6941	0.779	0.1772	−0.8586
15	130	13.07	−1.876	0.7906	0.7285	−0.0036	0.1283	−0.0283	0.589	0.0612	−0.0036
17	80	13.81	−5.502	0.6210	0.7426	−0.0996	0.1635	−0.6093	0.818	0.1604	0.1604
21	248	14.17	0.237	0.1196	0.2995	−0.0351	0.0929	−0.3780	1.143	0.4859	0.4789
22	126	7.03	0.680	0.5463	0.8569	0.0979	0.1303	0.7514	0.618	0.1290	−0.2775
23	100	17.05	−1.818	0.6127	0.7009	0.1398	0.1463	0.9560	0.468	0.0670	−0.0148
31	210	**33.70**	**15.978**	**0.0004**	**0.0022**	0.1371	0.1009	1.3586	**1.794**	**1.3340**	**1.0848**
41	192	22.78	6.538	0.0495	**0.0119**	−0.0040	0.1056	−0.0381	**1.371**	0.5135	**−0.4546**
42	230	24.65	−3.775	0.4007	0.4443	0.0556	0.0965	0.5768	0.747	0.2420	−0.5970
44	80	26.72	7.946	0.0472	0.0498	−0.2000	0.1635	−1.2230	1.336	0.4800	−0.1473
51	228	**29.64**	−0.409	0.0245	**0.0184**	0.0928	0.0969	0.9574	**1.443**	0.5956	0.5954
52	172	21.61	3.039	**0.0107**	0.0399	−0.2028	0.1115	−1.8187	**1.417**	**0.6913**	**0.6731**
53	260	13.32	−3.290	0.5558	0.8212	−0.0549	0.0907	−0.6048	0.620	0.0862	−0.0647
61	258	19.85	−3.128	0.8344	0.1754	−0.0487	0.0911	−0.5352	0.615	0.0900	−0.1735
64	102	**28.73**	−7.542	0.1803	0.4877	0.0804	0.1448	0.5551	0.836	0.2517	−0.2426

Table 2. Test for isotropy of the orientations of the galaxy plane. The distribution of the angle η of galaxies; inclination was taken directly from the NBG Catalog.

Group	N	χ^2	C	$P(\Delta_1)$	$P(\Delta)$	Δ_{11}	$\sigma(\Delta_{11})$	$\frac{\Delta_{11}}{\sigma(\Delta_{11})}$	λ	W^2	U^2
11	626	**60.01**	5.955	**0.0000**	**0.0000**	0.3040	0.0565	5.3782	**2.003**	**1.2774**	**1.2750**
12	332	**29.30**	**7.669**	**0.0013**	**0.0092**	−0.0686	0.0776	−0.8836	**1.756**	**0.9940**	**−0.7409**
13	128	25.56	2.781	0.0791	0.1048	0.2416	0.1250	1.9332	0.766	0.2142	−0.0221
14	426	27.38	6.634	0.0904	0.1476	0.0551	0.0685	0.8046	1.001	0.2964	−0.5861
15	130	22.86	2.508	0.7643	0.2086	0.0362	0.1240	0.2918	0.906	0.2649	0.2545
17	80	13.15	−5.975	0.4703	0.8201	−0.0590	0.1581	−0.3732	0.460	0.0467	0.0021
21	248	26.94	−3.548	0.0539	0.2016	0.0584	0.0898	0.6509	1.228	0.2912	−0.3671
22	126	11.71	5.571	0.1768	0.2239	0.1938	0.1260	1.5381	0.980	0.1935	0.1915
23	100	20.24	−0.100	0.0811	0.2323	−0.1644	0.1414	−1.1623	1.089	0.2968	0.2868
31	210	24.00	0.429	0.0455	0.0363	0.1940	0.0976	1.9882	**1.564**	**0.6733**	**0.6054**
41	192	27.19	**10.219**	**0.0009**	**0.0022**	0.3001	0.1021	2.9406	**1.949**	**0.8840**	**0.8075**
42	230	15.90	3.296	0.0335	0.0690	0.0363	0.0933	0.3890	1.238	0.5716	−0.4880
44	80	20.35	−3.050	0.2264	0.1385	0.1482	0.1581	0.9370	0.783	0.1229	−0.0206
51	228	**30.63**	−5.368	0.0416	0.1250	0.2175	0.0937	2.3223	1.148	0.3636	0.3633
52	172	**38.14**	**12.291**	**0.0012**	**0.0013**	0.2118	0.1078	1.9644	**1.923**	**1.1189**	**0.9322**
53	260	12.22	−8.277	0.8159	0.9486	0.0075	0.0877	0.0856	0.338	0.0229	−0.1903
61	258	23.72	−12.558	0.5492	0.5111	0.0912	0.0880	1.0362	0.643	0.0716	−0.0812
64	102	**50.12**	−3.529	**0.0024**	**0.0004**	0.4016	0.1400	2.8681	**1.881**	**1.4348**	**1.0276**

Table 3. Test for isotropy of the orientations of the galaxy plane. The distribution of the angle δ_D of galaxies; inclination was calculated on the basis of the value of the parameter q_0, depending on the morphological types of galaxies.

Group	N	χ^2	C	$P(\Delta_1)$	$P(\Delta)$	Δ_{11}	$\sigma(\Delta_{11})$	$\frac{\Delta_{11}}{\sigma(\Delta_{11})}$	λ	W^2	U^2
11	626	**57.92**	**23.719**	**0.0000**	**0.0000**	−0.2933	0.0585	−5.0172	**1.677**	**1.0639**	**0.7595**
12	332	19.86	4.313	0.0214	0.0845	−0.2191	0.0803	−2.7296	0.933	0.2848	−0.3688
13	128	21.74	−1.985	0.9017	0.7291	−0.0366	0.1293	−0.2831	0.533	0.0713	0.0309
14	426	**32.58**	5.004	0.0400	0.0967	−0.1722	0.0709	−2.4297	0.848	0.2398	−0.7484
15	130	11.19	−0.758	0.5857	0.7867	−0.0287	0.1283	−0.2235	0.676	0.1626	0.1623
17	80	9.12	−0.995	0.3735	0.6282	−0.1663	0.1635	−1.0171	0.818	0.1892	0.1871
21	248	23.79	**7.660**	**0.0141**	**0.0136**	−0.0726	0.0929	−0.7816	**1.479**	**1.0499**	**0.9137**
22	126	10.84	0.657	0.6402	0.7832	0.0186	0.1303	0.1425	0.668	0.1539	0.1539
23	100	12.33	−0.395	0.7644	0.8413	0.0620	0.1463	0.4238	0.768	0.1197	0.1174
31	210	**44.38**	**25.404**	**0.0000**	**0.0000**	0.1639	0.1009	1.6236	**2.346**	**2.5927**	**1.7750**
41	192	**27.61**	**8.682**	**0.0068**	**0.0031**	−0.0286	0.1056	−0.2714	**1.756**	**0.9233**	**−0.6765**
42	230	**32.77**	**9.035**	0.0333	**0.0111**	−0.0440	0.0965	−0.4559	**1.615**	**1.0730**	**−1.1977**
44	80	26.92	6.010	0.0843	0.0494	−0.1695	0.1635	−1.0366	1.336	0.3753	−0.1509
51	228	25.02	**8.541**	**0.0031**	**0.0036**	0.1017	0.0969	1.0493	**1.841**	**1.1469**	**1.0003**
52	172	**34.29**	**13.770**	**0.0001**	**0.0004**	−0.2716	0.1115	−2.4355	**2.059**	**1.3897**	**1.2726**
53	260	24.59	−8.649	0.1497	0.3568	−0.0173	0.0907	−0.1910	1.116	0.3326	0.3127
61	258	15.34	2.191	0.4203	0.2260	−0.0692	0.0911	−0.7596	0.778	0.2029	−0.5779
64	102	16.20	3.880	0.0686	0.2525	0.0967	0.1448	0.6675	1.174	0.5700	−0.3663

Table 4. Test for isotropy of the orientations of the galaxy plane. The distribution of the angle η of galaxies; inclination was calculated on the basis of the value of the parameter q_0 depending on the morphological types of galaxies.

Group	N	χ^2	C	$P(\Delta_1)$	$P(\Delta)$	Δ_{11}	$\sigma(\Delta_{11})$	$\frac{\Delta_{11}}{\sigma(\Delta_{11})}$	λ	W^2	U^2
11	626	**56.85**	**36.319**	**0.0000**	**0.0000**	0.3537	0.0565	6.2568	**2.243**	**1.6620**	**1.6619**
12	332	**42.75**	**21.169**	**0.0000**	**0.0000**	−0.0827	0.0776	−1.0655	**2.525**	**2.3969**	**−0.9833**
13	128	11.78	3.062	0.4461	0.2028	0.0761	0.1250	0.6086	0.687	0.0881	0.0152
14	426	**37.01**	6.169	**0.0028**	**0.0184**	0.1192	0.0685	1.7393	**2.003**	**0.8524**	**−0.9157**
15	130	15.11	1.538	0.9386	0.5245	0.0362	0.1240	0.2918	0.819	0.1946	0.1892
17	80	27.55	−4.175	0.0331	0.1025	−0.0693	0.1581	−0.4384	1.242	0.4029	0.3807
21	248	**32.74**	2.911	0.0233	0.0766	0.1423	0.0898	1.5846	**1.672**	0.5100	−0.5151
22	126	18.57	4.857	0.0283	0.0446	0.2867	0.1260	2.2756	1.336	0.4646	0.4329
23	100	**30.32**	1.880	**0.0028**	**0.0129**	−0.2230	0.1414	−1.5770	**1.500**	0.5953	0.5530
31	210	19.71	4.714	0.1124	0.0604	0.1546	0.0976	1.5847	1.426	0.6460	0.5611
41	192	**30.19**	**18.000**	**0.0001**	**0.0001**	0.3337	0.1021	3.2692	**2.165**	**1.3420**	**1.1144**
42	230	**29.20**	**8.774**	**0.0011**	**0.0023**	0.0056	0.0933	0.0601	**1.568**	**1.0667**	−0.4937
44	80	20.35	−3.500	0.1931	0.1889	−0.0166	0.1581	−0.1051	1.230	0.2769	−0.1731
51	228	27.32	−5.526	**0.0152**	0.0749	0.2658	0.0937	2.8376	1.038	0.3010	0.2699
52	172	**42.95**	**14.384**	**0.0001**	**0.0001**	0.2723	0.1078	2.5252	**1.999**	**1.4852**	**1.1819**
53	260	17.20	−8.346	0.8463	0.9801	0.0506	0.0877	0.5765	0.331	0.0288	−0.1908
61	258	14.23	1.395	0.0624	0.2010	0.0777	0.0880	0.8823	1.038	0.2738	−0.3536
64	102	**49.41**	**7.059**	**0.0004**	**0.0001**	0.4467	0.1400	3.1898	**2.145**	**1.5728**	**1.1656**

Table 5. Test for isotropy of the orientations of the galaxy plane. The distribution of the angle δ_D of galaxies; inclination was calculated on the basis of the value of the parameter $q_0 = 0.2$ adding 3°.

Group	N	χ^2	C	$P(\Delta_1)$	$P(\Delta)$	Δ_{11}	$\sigma(\Delta_{11})$	$\frac{\Delta_{11}}{\sigma(\Delta_{11})}$	λ	W^2	U^2
11	626	**40.50**	**9.005**	**0.0010**	**0.0029**	−0.2162	0.0585	−3.6976	1.117	0.5127	−0.2190
12	332	26.26	−10.374	0.2806	0.6207	−0.1266	0.0803	−1.5776	0.659	0.1273	−0.4848
13	128	**30.23**	−4.625	0.9468	0.6984	0.0284	0.1293	0.2196	0.709	0.0777	−0.0391
14	426	23.06	2.429	0.2470	0.2648	−0.1030	0.0709	−1.4527	0.671	0.1606	−0.8602
15	130	13.03	−2.190	0.9535	0.9219	0.0182	0.1283	0.1419	0.413	0.0334	−0.0864
17	80	11.69	−3.653	0.5899	0.7242	−0.1028	0.1635	−0.6288	0.818	0.1568	0.1567
21	248	14.35	−0.545	0.2296	0.3445	−0.0367	0.0929	−0.3949	0.953	0.3753	0.3751
22	126	7.19	1.262	0.5879	0.8853	0.0890	0.1303	0.6831	0.618	0.1265	−0.2792
23	100	9.84	1.101	0.6842	0.7517	0.1274	0.1463	0.8712	0.468	0.0590	0.0039
31	210	**35.10**	**12.811**	**0.0011**	**0.0050**	0.1452	0.1009	1.4387	**1.794**	**1.1787**	**0.9978**
41	192	19.23	**10.133**	0.0976	**0.0101**	0.0186	0.1056	0.1765	1.227	0.3955	−0.3974
42	230	22.75	−2.786	0.4480	0.4779	0.0426	0.0965	0.4414	0.731	0.2791	−0.6753
44	80	16.97	3.285	0.2003	0.2551	−0.1580	0.1635	−0.9659	0.894	0.2674	−0.1486
51	228	**28.26**	−0.982	0.0717	0.0408	0.0878	0.0969	0.9067	1.245	0.4125	0.4042
52	172	24.44	1.966	**0.0078**	0.0299	−0.2071	0.1115	−1.8568	**1.417**	**0.7238**	**0.7047**
53	260	13.23	−5.424	0.5904	0.7270	−0.0768	0.0907	−0.8468	0.496	0.0673	−0.1603
61	258	17.20	−6.559	0.9514	0.5678	−0.0125	0.0911	−0.1378	0.491	0.0480	−0.1855
64	102	23.89	−7.883	0.3004	0.6505	0.1192	0.1448	0.8232	0.737	0.1460	−0.1888

Table 6. Test for isotropy of the orientations of the galaxy plane. The distribution of the angle η of galaxies; inclination was calculated on the basis of the value of the parameter $q_0 = 0.2$ adding 3°.

Group	N	χ^2	C	$P(\Delta_1)$	$P(\Delta)$	Δ_{11}	$\sigma(\Delta_{11})$	$\frac{\Delta_{11}}{\sigma(\Delta_{11})}$	λ	W^2	U^2
11	626	**40.46**	3.137	**0.0001**	**0.0005**	0.2435	0.0565	4.3073	**1.603**	**0.7477**	**0.6802**
12	332	21.71	**7.235**	**0.0041**	0.0255	−0.0555	0.0776	−0.7154	**1.592**	**0.8543**	**−0.7237**
13	128	12.91	−0.313	0.8080	0.4251	0.0813	0.1250	0.6504	0.756	0.0885	0.0746
14	426	19.52	6.972	0.0690	0.1265	0.0727	0.0685	1.0616	1.034	0.3047	−0.5727
15	130	17.88	2.508	0.5804	0.2758	−0.0232	0.1240	−0.1871	0.906	0.3805	0.3258
17	80	13.60	−5.975	0.5065	0.8224	−0.0249	0.1581	−0.1577	0.460	0.0461	0.0041
21	248	24.61	−6.016	0.2029	0.5005	0.0590	0.0898	0.6565	1.101	0.2125	−0.4175
22	126	12.57	2.714	0.1768	0.2631	0.1849	0.1260	1.4675	0.980	0.1725	0.1670
23	100	17.36	1.880	0.0814	0.2286	−0.1751	0.1414	−1.2384	1.089	0.3724	0.3302
31	210	20.23	0.343	0.1140	0.0630	0.1528	0.0976	1.5657	**1.426**	0.5653	0.5141
41	192	**27.94**	**9.750**	**0.0016**	**0.0030**	0.3032	0.1021	2.9706	**1.732**	**0.6493**	**0.6384**
42	230	15.90	6.191	0.0283	0.0396	0.0266	0.0933	0.2854	1.172	0.6226	−0.4905
44	80	15.40	1.900	0.4251	0.1171	0.0399	0.1581	0.2524	0.671	0.0897	0.0080
51	228	21.63	−2.368	0.0611	0.2111	0.2101	0.0937	2.2437	1.148	0.3162	0.3148
52	172	**36.67**	**14.802**	**0.0015**	**0.0015**	0.2082	0.1078	1.9304	**1.847**	**1.0693**	**0.8969**
53	260	11.80	−2.600	0.5311	0.7438	0.0522	0.0877	0.5953	0.531	0.0563	−0.0874
61	258	18.98	−10.116	0.5731	0.8244	0.0469	0.0880	0.5328	0.664	0.0420	−0.2271
64	102	**45.88**	5.471	**0.0023**	**0.0001**	0.3941	0.1400	2.8144	**1.980**	**1.4383**	**1.0381**

This fact obliges us to choose the best method of calculating the angle of inclination used in the new research method. Therefore, when calculating the new "theoretical isotropic distributions", various variants of calculating the angle of inclination were considered. The original Holmberg's Formula (6), Tully's approach (7), as well as two variations of these methods, were taken into account.

Figures 3–10 show a comparison of these variants in terms of calculating the angle of inclination for four Tully groups unrelated to the direction toward the LSC center. For comparison, next to three sufficiently numerous groups (12, 42, 53), one less numerous group (17) was selected. It turned out that adding 3° to the calculated angle of inclination leads to a noticeable change in the distribution of the calculated angles δ_D and η. In its original assumption, as used by Tully, for example, the addition of 3° was intended to

compensate for not taking into account the morphological types of galaxies. The obtained distributions show that this approach may not meet expectations.

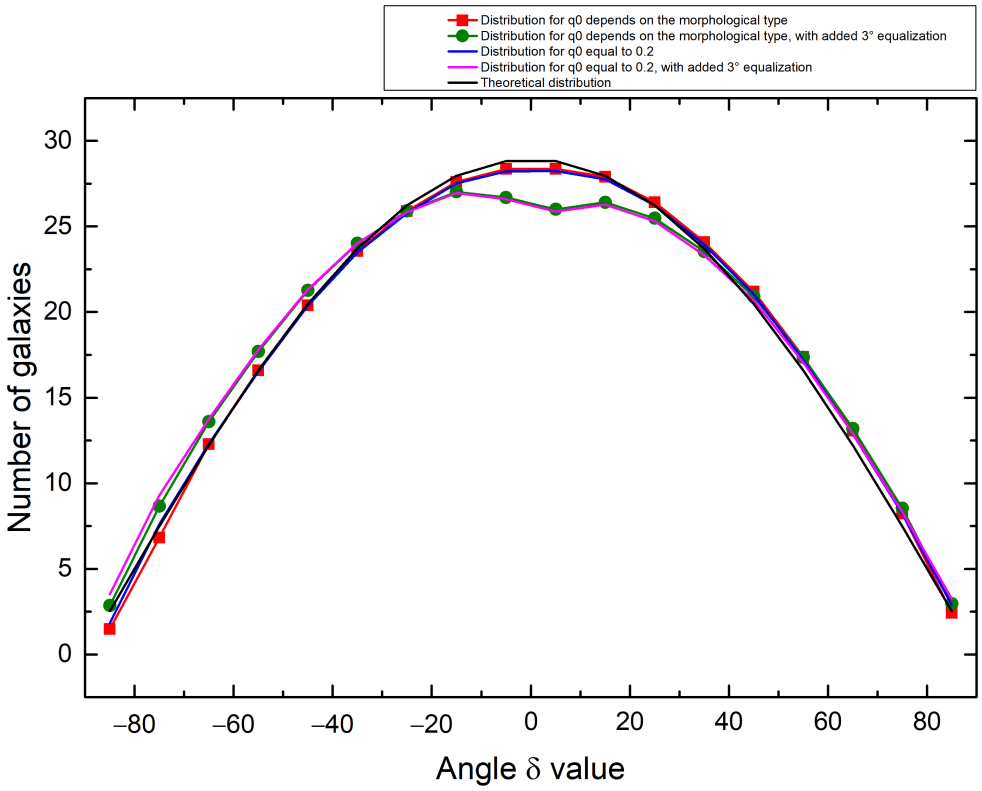


Figure 3. Simulated distributions of the angle δ_D for group 12.

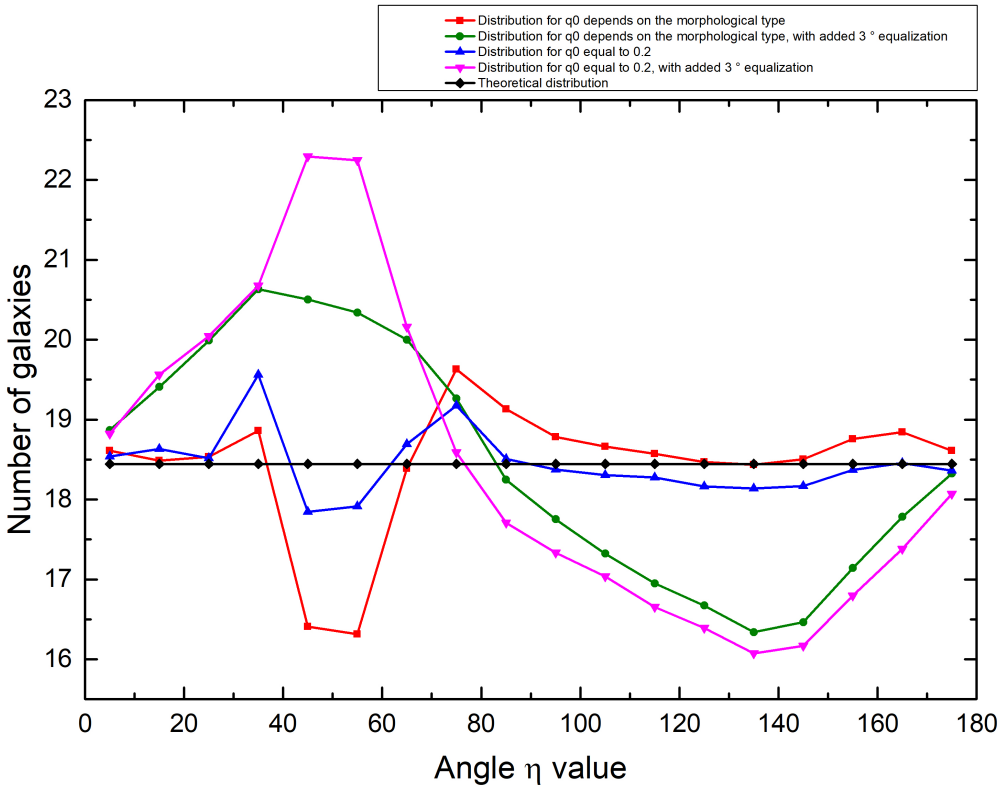


Figure 4. Simulated distributions of the angle η for group 12.

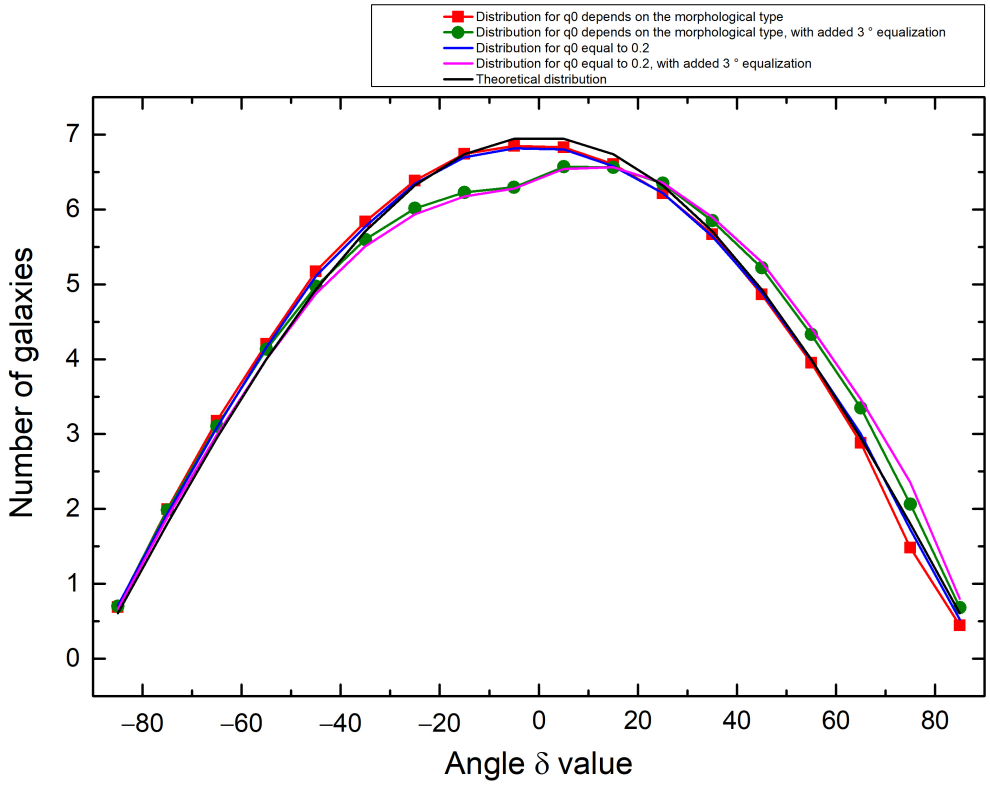


Figure 5. Simulated distributions of the angle δ_D for group 17.

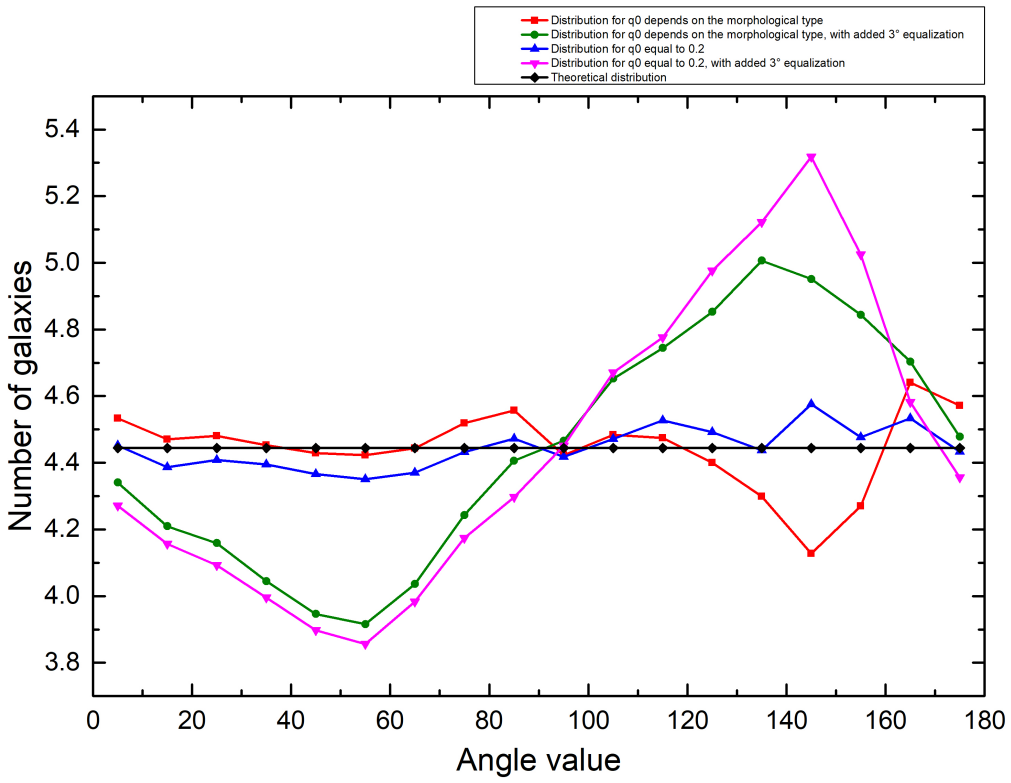


Figure 6. Simulated distributions of the angle η for group 17.

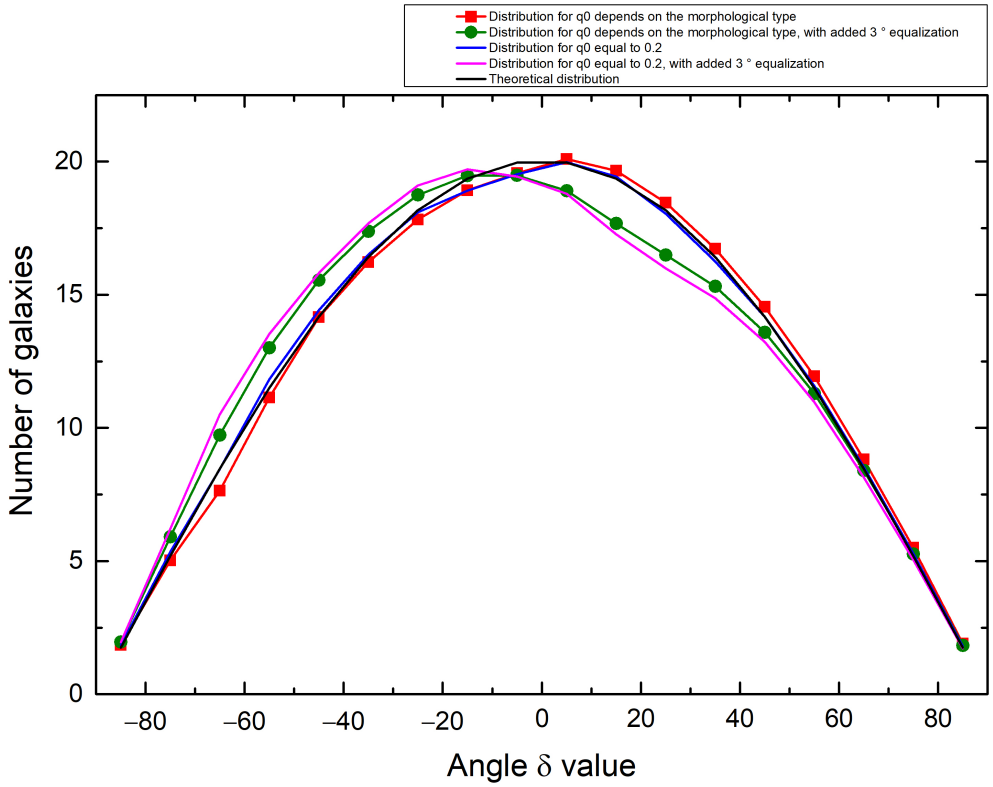


Figure 7. Simulated distributions of the angle δ_D for group 42.

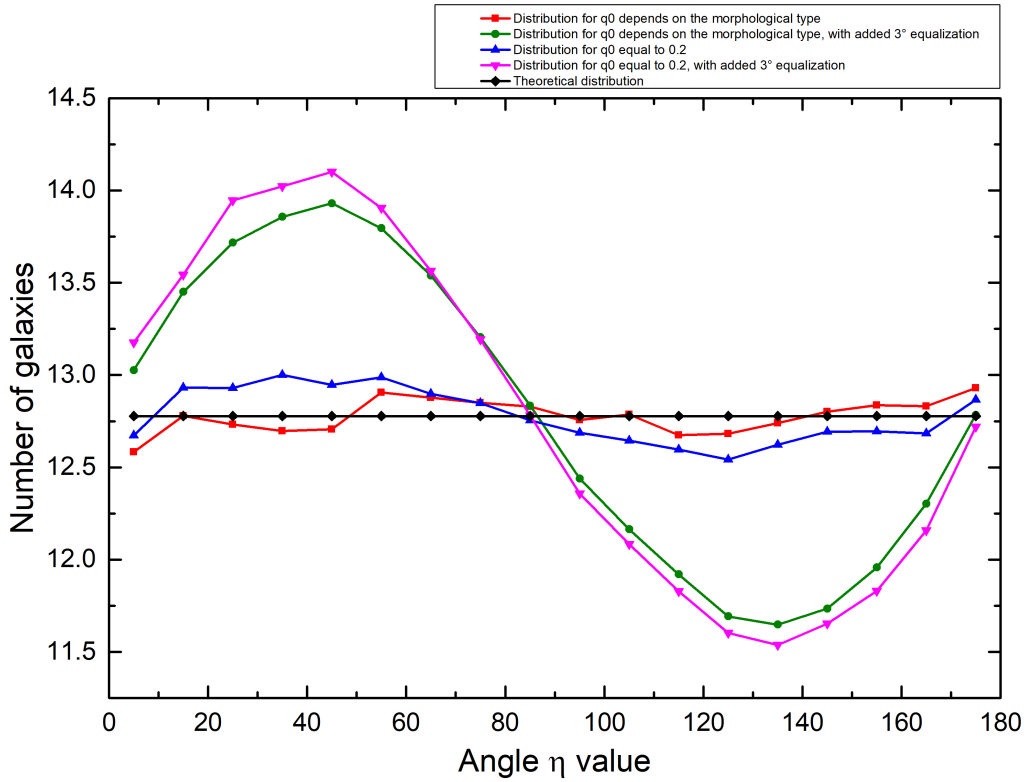


Figure 8. Simulated distributions of the angle η for group 42.

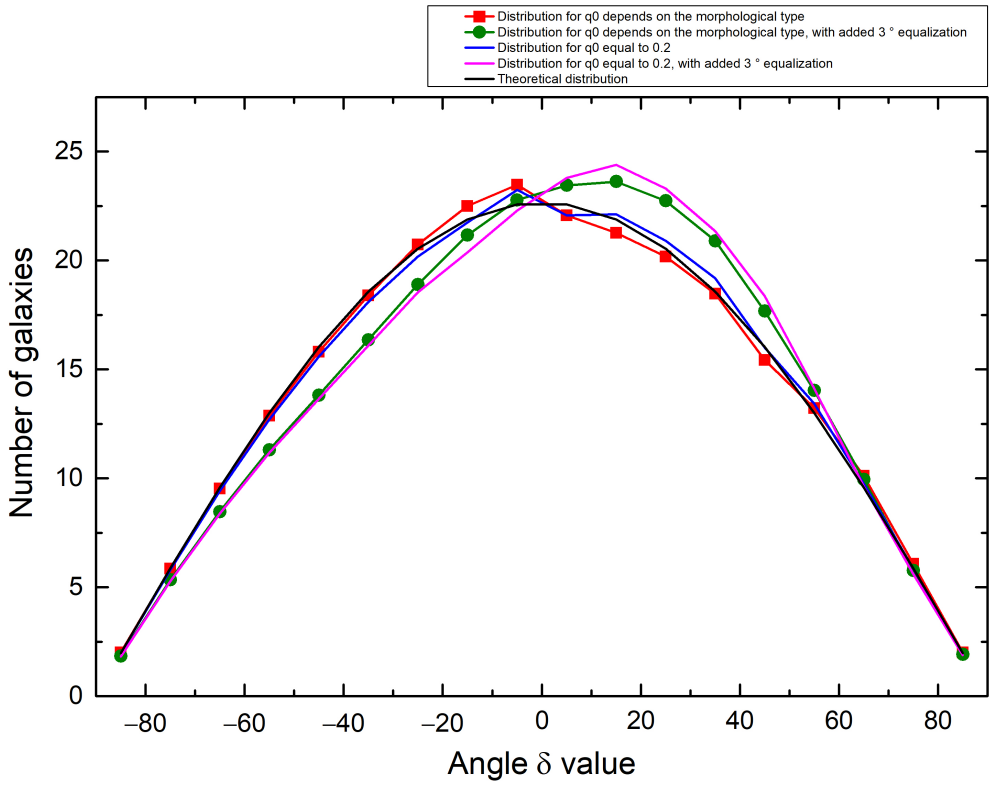


Figure 9. Simulated distributions of the angle δ_D for group 53.

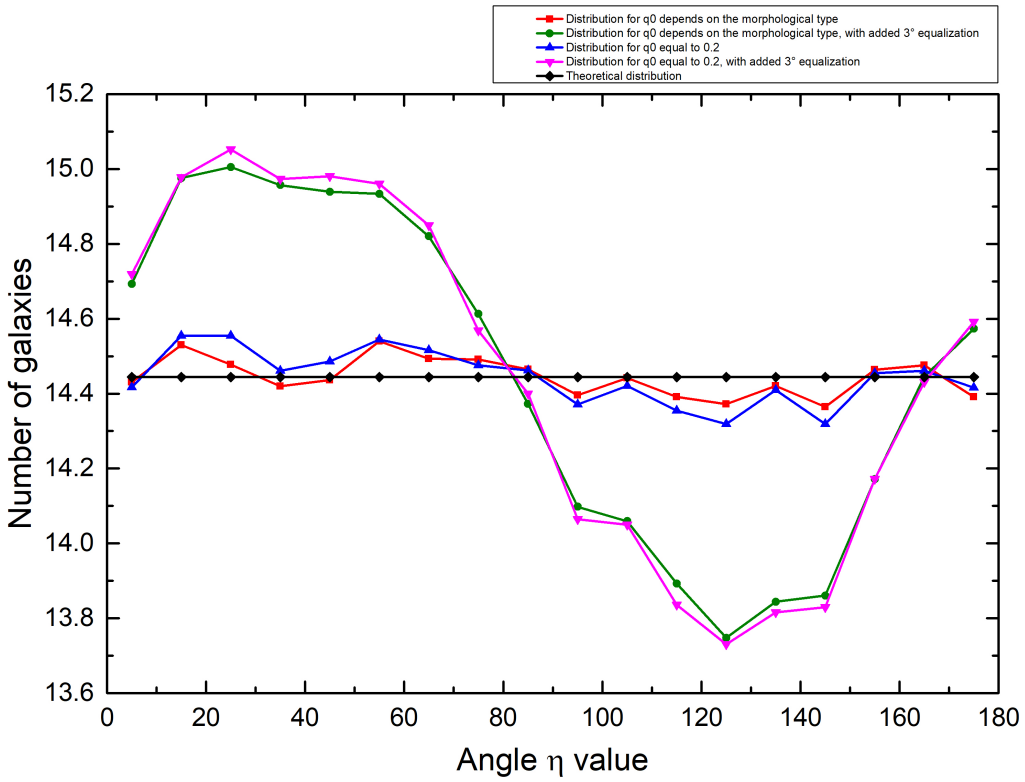


Figure 10. Simulated distributions of the angle η for group 53.

As part of the calculation of the new "theoretical isotropic distributions", 10,000 simulations of fictitious galaxies were performed for each group in the Tully Catalog. The results of these simulations are presented in Tables 7–10. These tables contain the mean

values (for 10,000 simulations) of the statistical tests of the δ_D and η angles, as well as the standard deviations of these values. They present the results of statistical tests for isotropic distributions of δ_D and η angles simulated using our method (assuming that the distribution of galaxy orientations in space is isotropic). The end result of the simulation was obtaining new "theoretical isotropic distributions". Verification of the effectiveness of the proposed new research method is possible by calculating new statistical tests using "theoretical isotropic distributions" obtained from numerical simulations. Tables 11 and 12 present the results of the analysis for the real distributions of δ_D and η angles, taking into account their morphological types. The same experimental data were used in the calculation of the statistical tests presented in Tables 3, 4, 11 and 12. The difference was that, in the case of Tables 3 and 4, information on the morphological type of each galaxy was used separately, and in Tables 11 and 12, a simulated "theoretical isotropic distribution" was used, which already took into account the information on morphological types. This means that, in the second case, simulated distributions was used instead of ideal theoretical isotropic distributions (i.e., cosine distribution in the case of δ_D angle, and uniform distribution in the case of η angle) Comparison of the results obtained in both cases shows that the alignment was obtained for the same groups.

Table 7. Result of the numerical simulations—mean values of δ_D angle statistical tests with standard deviations—part 1.

Group	N	χ^2	$\sigma(\chi^2)$	C	$\sigma(C)$	λ	$\sigma(\lambda)$	W^2	$\sigma(W^2)$	U^2	$\sigma(U^2)$
11	626	17.88	7.01	−0.410	4.756	0.646	0.202	0.1210	0.0820	−0.3606	0.1580
12	332	17.04	6.78	−0.634	4.557	0.612	0.192	0.1091	0.0747	−0.4693	0.1320
13	128	17.62	6.97	−0.851	4.627	0.648	0.208	0.1252	0.0892	0.0487	0.1291
14	426	16.97	6.26	−0.758	4.276	0.638	0.211	0.1216	0.0864	−0.5227	0.2569
15	130	17.45	6.39	−0.593	4.385	0.732	0.285	0.1835	0.1776	−0.0160	0.2446
17	80	17.24	6.58	−0.961	4.410	0.629	0.211	0.1183	0.0894	0.0492	0.1213
21	248	17.40	6.24	−0.617	4.404	0.728	0.286	0.1830	0.1790	−0.1209	0.3277
22	126	17.52	6.46	−0.476	4.477	0.713	0.269	0.1695	0.1553	0.0001	0.2211
23	100	17.22	6.41	−0.698	4.310	0.649	0.217	0.1266	0.0959	0.0334	0.1419
31	210	17.21	6.10	−0.646	4.178	0.768	0.316	0.2143	0.2262	−0.1733	0.3613
41	192	17.56	6.37	−0.590	4.447	0.739	0.292	0.1837	0.1747	−0.1945	0.2968
42	230	17.59	6.34	−0.560	4.433	0.718	0.267	0.1676	0.1466	−0.2908	0.2841
44	80	17.31	6.29	−0.692	4.271	0.759	0.313	0.2052	0.2111	−0.0070	0.2206
51	228	17.26	6.19	−0.614	4.238	0.770	0.326	0.2193	0.2307	−0.1817	0.3801
52	172	17.31	6.23	−0.655	4.401	0.705	0.253	0.1608	0.1381	−0.0247	0.2365
53	260	17.34	6.12	−0.588	4.192	0.769	0.314	0.2142	0.2209	−0.2262	0.3967
61	258	17.34	6.19	−0.644	4.291	0.679	0.234	0.1424	0.1097	−0.3296	0.2494
64	102	17.29	6.29	−0.549	4.293	0.751	0.294	0.1944	0.1885	−0.0508	0.2340

Table 8. Result of the numerical simulations—mean values of δ_D angle statistical tests with standard deviations—part 2.

Group	N	$P(\Delta_1)$	$\sigma(P(\Delta_1))$	$P(\Delta)$	$\sigma(P(\Delta))$	Δ_{11}	$\sigma(\Delta_{11})$	$\frac{\Delta_{11}}{\sigma(\Delta_{11})}$	$\sigma(\frac{\Delta_{11}}{\sigma(\Delta_{11})})$
11	626	0.5730	0.2938	0.5587	0.3181	0.0068	0.0717	0.1156	1.2271
12	332	0.5877	0.2976	0.5748	0.3117	0.0049	0.0981	0.0605	1.2217
13	128	0.5716	0.2900	0.5597	0.3086	0.0082	0.1533	0.0636	1.1860
14	426	0.5612	0.2868	0.5538	0.2953	0.0064	0.0807	0.0905	1.1389
15	130	0.5205	0.2952	0.5104	0.2987	0.0072	0.1239	0.0560	0.9657
17	80	0.5787	0.2937	0.5678	0.3035	0.0057	0.1910	0.0347	1.1681

Table 8. *Cont.*

Group	N	$P(\Delta_1)$	$\sigma(P(\Delta_1))$	$P(\Delta)$	$\sigma(P(\Delta))$	Δ_{11}	$\sigma(\Delta_{11})$	$\frac{\Delta_{11}}{\sigma(\Delta_{11})}$	$\sigma(\frac{\Delta_{11}}{\sigma(\Delta_{11})})$
21	248	0.5286	0.2963	0.5156	0.3004	0.0053	0.0873	0.0566	0.9404
22	126	0.5343	0.2968	0.5171	0.3034	0.0077	0.1357	0.0594	1.0417
23	100	0.5691	0.2914	0.5491	0.3007	0.0048	0.1686	0.0331	1.1527
31	210	0.5009	0.2962	0.4995	0.2920	0.0037	0.0722	0.0371	0.7149
41	192	0.5200	0.2973	0.5088	0.3005	0.0044	0.0997	0.0413	0.9448
42	230	0.5272	0.2929	0.5152	0.2988	0.0070	0.1004	0.0721	1.0406
44	80	0.5060	0.2982	0.5060	0.2969	0.0050	0.1289	0.0303	0.7884
51	228	0.5042	0.299	0.5061	0.2967	0.0030	0.0661	0.0309	0.6821
52	172	0.5294	0.2914	0.5185	0.2954	0.0053	0.1183	0.0477	1.0609
53	260	0.4989	0.2971	0.4938	0.2972	0.0034	0.0674	0.0375	0.7428
61	258	0.5467	0.2902	0.5287	0.2953	0.0049	0.1008	0.0536	1.1066
64	102	0.5076	0.2944	0.5045	0.2968	0.0072	0.1260	0.0497	0.8699

Table 9. Result of the numerical simulations—mean values of η angle statistical tests with standard deviations—part 1.

Group	N	χ^2	$\sigma(\chi^2)$	C	$\sigma(C)$	λ	$\sigma(\lambda)$	W^2	$\sigma(W^2)$	U^2	$\sigma(U^2)$
11	626	18.11	6.38	−0.449	4.335	0.706	0.237	0.1424	0.1113	−0.3902	0.3356
12	332	17.22	6.01	−0.861	4.145	0.760	0.299	0.1882	0.1900	−0.2306	0.3157
13	128	16.65	5.81	−1.055	3.987	0.748	0.290	0.1839	0.1832	−0.0250	0.2040
14	426	16.98	5.96	−0.898	4.061	0.741	0.275	0.1732	0.1653	−0.2386	0.3469
15	130	16.72	5.73	−0.932	3.968	0.732	0.264	0.1686	0.1572	−0.0175	0.1935
17	80	16.51	5.69	−1.013	3.919	0.745	0.291	0.1834	0.1859	0.0247	0.1751
21	248	16.86	5.74	−1.020	4.049	0.735	0.266	0.1701	0.1567	−0.0984	0.2643
22	126	16.73	5.77	−1.025	4.045	0.740	0.285	0.1789	0.1762	−0.0223	0.2019
23	100	17.07	6.13	−1.197	4.301	0.745	0.306	0.1855	0.1958	0.0225	0.1988
31	210	17.75	6.08	−0.295	4.342	0.791	0.296	0.2027	0.1921	−0.0656	0.2705
41	192	16.60	5.71	−0.926	4.046	0.734	0.273	0.1718	0.1635	−0.0693	0.2363
42	230	16.65	5.89	−1.093	3.999	0.741	0.281	0.1768	0.1719	−0.1016	0.2667
44	80	17.12	5.81	−0.700	4.100	0.763	0.283	0.1855	0.1769	0.0295	0.1686
51	228	17.31	5.92	−0.524	4.253	0.759	0.275	0.1842	0.1683	−0.0867	0.2620
52	172	16.65	5.71	−1.027	4.028	0.722	0.265	0.1635	0.1534	−0.0560	0.2190
53	260	17.65	6.00	−0.305	4.291	0.786	0.288	0.1960	0.1801	−0.0954	0.2919
61	258	16.64	5.62	−1.062	3.925	0.735	0.271	0.1728	0.1629	−0.1203	0.2733
64	102	16.92	5.84	−0.793	4.011	0.747	0.275	0.1788	0.1676	0.0102	0.1832

Table 10. Result of the numerical simulations—mean values of η angle statistical tests with standard deviations—part 2.

Group	N	$P(\Delta_1)$	$\sigma(P(\Delta_1))$	$P(\Delta)$	$\sigma(P(\Delta))$	Δ_{11}	$\sigma(\Delta_{11})$	$\frac{\Delta_{11}}{\sigma(\Delta_{11})}$	$\sigma(\frac{\Delta_{11}}{\sigma(\Delta_{11})})$
11	626	0.5127	0.3044	0.4647	0.3027	0.0226	0.0676	0.4004	1.1968
12	332	0.5164	0.2935	0.5019	0.2957	−0.0021	0.0552	−0.0276	0.7107
13	128	0.5108	0.2902	0.5137	0.2896	0.0040	0.0980	0.0321	0.7841
14	426	0.5100	0.2928	0.5013	0.2942	0.0054	0.0660	0.0795	0.9630
15	130	0.4947	0.2886	0.4992	0.2878	0.0002	0.1217	0.0013	0.9810
17	80	0.5218	0.2918	0.5218	0.2911	0.0009	0.1131	0.0059	0.7154
21	248	0.4954	0.2921	0.5029	0.2906	−0.0026	0.0924	−0.0284	1.0285
22	126	0.5071	0.2942	0.5077	0.2927	0.0003	0.1212	0.0025	0.9624
23	100	0.5432	0.3079	0.5252	0.3054	−0.0065	0.1084	−0.0462	0.7668
31	210	0.4386	0.2948	0.4384	0.2931	0.0021	0.1064	0.0220	1.0905
41	192	0.5026	0.2914	0.5044	0.2908	−0.0024	0.1046	−0.0239	1.0251
42	230	0.5010	0.2897	0.5097	0.2883	−0.0013	0.0826	−0.0140	0.8856
44	80	0.4679	0.2942	0.4725	0.2887	0.0013	0.1565	0.0079	0.9900

Table 10. *Cont.*

Group	N	$P(\Delta_1)$	$\sigma(P(\Delta_1))$	$P(\Delta)$	$\sigma(P(\Delta))$	Δ_{11}	$\sigma(\Delta_{11})$	$\frac{\Delta_{11}}{\sigma(\Delta_{11})}$	$\sigma(\frac{\Delta_{11}}{\sigma(\Delta_{11})})$
51	228	0.4623	0.2966	0.4635	0.2949	−0.0053	0.1083	−0.0561	1.1565
52	172	0.5159	0.2943	0.5147	0.2925	−0.0002	0.1134	−0.0018	1.0520
53	260	0.4369	0.2941	0.4410	0.2937	−0.0013	0.0968	−0.0143	1.1042
61	258	0.5017	0.2887	0.5100	0.2884	0.0060	0.0788	0.0681	0.8944
64	102	0.4858	0.2958	0.4876	0.2923	−0.0024	0.1505	−0.0175	1.0747

Table 11. Test for isotropy of the orientations of the galaxy plane. The distribution of the angle δ_D of galaxies was obtained using the new "theoretical isotropic distribution" calculated for q_0, depending on the morphological type.

Group	N	χ^2	C	$P(\Delta_1)$	$P(\Delta)$	Δ_{11}	$\sigma(\Delta_{11})$	$\frac{\Delta_{11}}{\sigma(\Delta_{11})}$	λ	W^2	U^2
11	626	**59.24**	**23.837**	**0.0000**	**0.0000**	−0.3015	0.0588	−5.1272	1.340	**0.9076**	0.0284
12	332	23.51	0.701	0.0346	0.1072	−0.2091	0.0807	−2.5897	0.879	0.2563	−0.2613
13	128	22.40	−2.716	0.9304	0.8442	−0.0388	0.1300	−0.2988	0.405	0.0473	−0.1276
14	426	26.87	6.327	0.0358	0.1166	−0.1767	0.0712	−2.4833	0.900	0.2252	−0.6374
15	130	9.52	−1.566	0.7928	0.8999	−0.0054	0.1283	−0.0421	0.603	0.0975	0.0884
17	80	8.26	−2.106	0.5284	0.6738	−0.1596	0.1644	−0.9710	0.722	0.1157	0.1095
21	248	20.46	1.613	0.0446	0.0695	−0.0705	0.0928	−0.7591	1.267	0.7711	0.7104
22	126	6.81	−2.527	0.9384	0.9975	0.0267	0.1305	0.2046	0.224	0.0095	−0.1159
23	100	10.41	1.246	0.8812	0.8719	0.0692	0.1468	0.4713	0.438	0.0418	−0.0487
31	210	**36.41**	**19.094**	**0.0000**	**0.0001**	0.1678	0.1007	1.6666	**2.163**	**2.0593**	**1.5171**
41	192	**27.75**	**11.562**	**0.0069**	**0.0017**	−0.0289	0.1055	−0.2741	**1.804**	**0.9063**	**−0.6480**
42	230	**30.49**	3.900	0.1172	0.0522	−0.0416	0.0966	−0.4311	1.269	0.6391	**−0.9776**
44	80	23.95	5.304	0.1277	0.1055	−0.1613	0.1629	−0.9902	1.213	0.3297	−0.1475
51	228	**30.51**	**7.548**	**0.0021**	**0.0013**	0.0899	0.0964	0.9328	**1.901**	**1.3166**	**1.0980**
52	172	**32.83**	**9.707**	**0.0006**	**0.0019**	−0.2640	0.1117	−2.3634	**1.841**	**1.0431**	**1.0122**
53	260	21.10	−8.961	0.2312	0.5331	−0.0388	0.0904	−0.4288	0.715	0.2149	0.1665
61	258	14.47	1.584	0.6123	0.3232	−0.0641	0.0913	−0.7016	0.638	0.1630	−0.5230
64	102	15.93	0.741	0.2564	0.6032	0.0964	0.1446	0.6663	0.904	0.2979	−0.3018

Table 12. Test for isotropy of the orientations of the galaxy plane. The distribution of the angle η of galaxies was obtained using the new "theoretical isotropic distribution" calculated for q_0, depending on the morphological type.

Group	N	χ^2	C	$P(\Delta_1)$	$P(\Delta)$	Δ_{11}	$\sigma(\Delta_{11})$	$\frac{\Delta_{11}}{\sigma(\Delta_{11})}$	λ	W^2	U^2
11	626	**51.09**	**34.516**	**0.0000**	**0.0000**	0.3406	0.0570	5.9768	**2.083**	**1.4864**	**1.4824**
12	332	**38.26**	**14.673**	**0.0000**	**0.0002**	−0.0708	0.0770	−0.9197	**2.096**	**1.5317**	**−0.7605**
13	128	14.28	−3.196	0.5306	0.2900	0.0919	0.1244	0.7387	0.482	0.0908	−0.0924
14	426	**30.46**	2.379	0.0113	0.0521	0.1018	0.0685	1.4850	**1.801**	**0.8471**	**−0.9937**
15	130	14.22	−0.256	0.8737	0.6347	0.0559	0.1239	0.4512	0.723	0.1404	0.1404
17	80	**34.01**	−15.640	0.1415	0.4103	−0.0651	0.1572	−0.4143	0.990	0.2576	0.2576
21	248	**33.80**	3.921	0.0289	0.1073	0.1186	0.0898	1.3207	**1.630**	0.5451	−0.5519
22	126	18.46	7.166	0.0417	0.0353	0.2560	0.1260	2.0310	1.357	0.4754	0.4349
23	100	27.23	5.659	**0.0041**	**0.0111**	−0.1985	0.1409	−1.4084	**1.571**	**0.7560**	**0.6315**
31	210	18.66	4.842	0.1164	0.0629	0.1541	0.0975	1.5796	1.289	0.4804	0.4539
41	192	**30.01**	**18.142**	**0.0001**	**0.0002**	0.3595	0.1021	3.5205	**2.036**	**1.0864**	**0.9845**
42	230	**32.96**	6.630	**0.0015**	**0.0015**	−0.0162	0.0932	−0.1739	**1.603**	**1.0393**	−0.5294
44	80	19.60	−1.483	0.2254	0.1314	0.0048	0.1581	0.0304	1.120	0.1952	−0.1201
51	228	26.59	−2.132	**0.0070**	0.0381	0.2885	0.0937	3.0789	1.184	0.3519	0.3292
52	172	**42.00**	**16.865**	**0.0001**	**0.0002**	0.2685	0.1078	2.4900	**2.021**	**1.4674**	**1.1505**
53	260	11.53	−5.162	0.8673	0.9880	0.0456	0.0877	0.5196	0.266	0.0230	−0.1978
61	258	10.94	2.142	0.1072	0.3355	0.0747	0.0880	0.8492	1.012	0.2731	−0.4037
64	102	**52.33**	2.005	**0.0009**	**0.0001**	0.4370	0.1401	3.1199	**2.149**	**1.5422**	**1.1508**

The next step is to take into account not only the effect of different q_0 values depending on the morphological type, but also to convert q to the standard photometrical axial ratios according to Fouque and Paturel formulae [35]. Our results are presented in Tables 13 and 14. It is easy to see that the strong anisotropy effect in the alignment of galaxies, observed when the values of the inclination angles were taken as the original values from the NBG catalog, now disappears. Looking at the results of the test statistics (Tables 13 and 14), we can see that for any group except the 11 Virgo cluster, the distribution of the angle η cannot be seen to significantly deviate from the values of the statistics predicted for random distributions. For the δ_D angle distributions, the largest deviation from the random distribution is observed for the 15 and 31 groups, but the effect is statistically marginal. As a result, we could conclude that when we analyzed the spatial orientation of galaxies inside 18 Tully groups of galaxies belonging to the Local Supercluster, taking into account their morphological type and FP correction, we do not find any significant alignment. This result indicates that the orientation of galaxies in the studied Tully groups is random.

The observational effect generated by the process of deprojection of galaxies from their optical images [47] makes it much harder to find real alignment during analysis of the spatial orientation of galaxies in clusters, but can be analyzed in more detail. For each δ_D angle for each cluster, we computed the Δ_{11} parameter, describing the galactic axes' alignment with respect to a chosen cluster pole, divided by its formal error $\sigma(\Delta_{11})$. It is called the s parameter, $s \equiv \Delta_{11}/\sigma(\Delta_{11}))$ [47]. The idea is to change the position of the coordinate system's pole along the entire celestial sphere. Thus, the main plane of the system also changes its position. For each such instantaneous coordinate system, we now compute the parameter s. The positive value of this coefficient means predominance of the normal perpendicular to the main plane, i.e., directed to the pole of the instantaneous coordinate system. The resulting maps can be also analyzed in terms of their correlations of their maxima with the important points on the maps.

In the Figure 11, we present analysis for Cluster 12 (Ursa Major Cloud). We choose this cluster because his position is far from the center of the Local Supercluster (i.e., Virgo Cluster), and thus avoids the possible influence of global alignment within the Local Supercluster In the left panel of this figure (i.e., for original inclination angles from NBG Catalogue), we observe strong maxima that correlate well with the direction of the line of sight. In this figure, we also mark other important points, such as the three possible poles of the cluster. There are three possible poles because Tully's catalog gives the affiliation (or not) of each galaxy in the catalog to galaxy groups, as well as spherical coordinates and independent distances for each galaxy. This means that we can obtain a three-dimensional spatial distribution of galaxies belonging to each studied group in terms of their Cartesian coordinates. Assuming a Gaussian distribution of positions in the cluster, we can thus fit the ellipsoid of covariance, and, thus, the directions of the three axes of the ellipsoid in space, which is a more general solution than adopting a simplified model, in which galaxy clusters are ellipsoids of rotation. The positions of these axes of the ellipsoid uniquely determine the positions of the three possible poles of the cluster. However, the observed maxima are not correlated with them.

It is easy, on the right panel (i.e., for the situation when we take into account their morphological types when calculating inclination angles and apply Fouque and Paturel corrections), to see that these maxima disappear. This confirms our opinion that the originally observed effect was not the result of a real alignment, but an effect related to not taking into account the real flattening of galaxies depending on their morphological types and the Fouque and Paturel correction. We would like to point out that the discussed method makes it possible to find even a weak alignment of galaxies in clusters. The example of cluster 15 illustrates this. The corresponding maps are shown on Figure 12. In this figure, we can find for the s parameter a 2σ maximum, which is uncorrelated with line-of-sight for all of the galaxy samples, and is a statistically weak result. However, for spiral galaxies, this effect is already at 3σ, with the maximum agreeing with the direction of the maximum

for all galaxies. This entitles us to conclude that for the spiral galaxies belonging to this cluster, we observe a real alignment.

Table 13. Test for isotropy of the orientations of the galaxy plane. The distribution of the angle δ_D was calculated with q_0 depending on the morphological type and Fouque and Paturel correction.

Group	N	χ^2	C	$P(\Delta_1)$	$P(\Delta)$	Δ_{11}	$\sigma(\Delta_{11})$	$\frac{\Delta_{11}}{\sigma(\Delta_{11})}$	λ	W^2	U^2
11	626	29.10	−5.254	0.3443	0.4907	−0.0761	0.0585	−1.3019	0.677	0.0710	−0.5891
12	332	12.72	−4.261	0.6408	0.9215	−0.0751	0.0803	−0.9354	0.384	0.0455	−0.3625
13	128	27.84	2.881	0.1580	0.0280	0.2268	0.1293	1.7539	0.786	0.2241	0.0307
14	426	19.25	6.103	0.9108	0.0589	0.0000	0.0709	0.0004	0.623	0.1024	−0.7387
15	130	23.10	−7.212	0.5977	0.6819	0.1024	0.1283	0.7986	0.789	0.0932	−0.2091
17	80	5.58	0.524	0.8311	0.7163	0.0242	0.1635	0.1480	0.559	0.0890	0.0890
21	248	19.39	−6.411	0.6978	0.4134	0.0265	0.0929	0.2852	0.889	0.1671	0.1328
22	126	14.82	3.054	0.6707	0.7872	0.0879	0.1303	0.6748	0.707	0.1110	−0.1888
23	100	17.97	−1.012	0.2056	0.3434	0.2343	0.1463	1.6021	0.614	0.1435	−0.0934
31	210	31.90	−0.093	0.0887	0.1243	0.1252	0.1009	1.2399	0.966	0.2677	0.2560
41	192	11.74	5.787	0.2636	0.1864	0.1102	0.1056	1.0443	0.722	0.2679	−0.4889
42	230	17.49	4.119	0.4208	0.0946	0.1201	0.0965	1.2447	0.786	0.1954	−0.4389
44	80	12.06	0.588	0.1610	0.4258	−0.1710	0.1635	−1.0457	0.900	0.2598	−0.2228
51	228	17.44	−4.402	0.6561	0.8442	0.0662	0.0969	0.6832	0.552	0.0833	0.0054
52	172	17.94	5.950	0.0082	0.0450	−0.1677	0.1115	−1.5040	1.454	0.7803	0.7109
53	260	9.79	−0.320	0.7056	0.8484	−0.0633	0.0907	−0.6983	0.523	0.0901	−0.5060
61	258	15.76	0.848	0.3385	0.2690	0.0710	0.0911	0.7796	0.802	0.1902	0.1498
64	102	19.78	−0.098	0.5297	0.6798	0.0697	0.1448	0.4813	0.594	0.0868	−0.1816

Table 14. Test for isotropy of the orientations of the galaxy plane. The distribution of the angle η was calculated with q_0 depending on the morphological type and Fouque and Paturel correction.

Group	N	χ^2	C	$P(\Delta_1)$	$P(\Delta)$	Δ_{11}	$\sigma(\Delta_{11})$	$\frac{\Delta_{11}}{\sigma(\Delta_{11})}$	λ	W^2	U^2
11	626	36.84	14.121	0.0009	0.0001	0.2020	0.0565	3.5736	1.101	0.4450	0.0557
12	332	17.37	2.464	0.4599	0.4165	−0.0462	0.0776	−0.5950	0.860	0.2365	−0.5615
13	128	17.12	6.297	0.4194	0.0529	0.1510	0.1250	1.2083	1.110	0.2416	0.2405
14	426	14.96	0.338	0.2655	0.3551	0.0321	0.0685	0.4685	0.775	0.1649	−0.5359
15	130	13.72	2.092	0.6530	0.2863	0.0164	0.1240	0.1324	0.643	0.1576	0.1575
17	80	9.10	0.550	0.7567	0.7188	−0.0213	0.1581	−0.1347	0.683	0.1061	0.1052
21	248	17.35	−4.710	0.7749	0.7616	−0.0028	0.0898	−0.0306	0.564	0.0917	0.0438
22	126	16.57	−2.571	0.9707	0.4506	0.0216	0.1260	0.1717	0.535	0.0286	−0.0656
23	100	10.16	−0.820	0.5729	0.8232	−0.1210	0.1414	−0.8555	0.444	0.0477	−0.0294
31	210	17.31	−0.514	0.3238	0.2418	0.1239	0.0976	1.2698	1.104	0.3029	0.3005
41	192	24.38	0.375	0.0181	0.0228	0.2685	0.1021	2.6307	0.962	0.2555	0.1976
42	230	16.05	0.478	0.4551	0.2283	−0.0077	0.0933	−0.0830	0.879	0.2468	−0.4326
44	80	14.05	1.000	0.8306	0.1871	0.0644	0.1581	0.4073	0.472	0.0678	0.0524
51	228	28.58	0.158	0.2769	0.1317	0.1375	0.0937	1.4683	1.214	0.4058	0.3993
52	172	17.63	4.651	0.0161	0.0758	0.1180	0.1078	1.0947	1.339	0.6194	0.5459
53	260	14.85	−4.192	0.3857	0.6592	0.0099	0.0877	0.1130	0.675	0.0943	0.0221
61	258	11.86	0.977	0.3174	0.2960	0.1159	0.0880	1.3159	0.955	0.2249	0.2211
64	102	12.71	2.118	0.1482	0.4019	0.2528	0.1400	1.8053	0.627	0.1198	0.0714

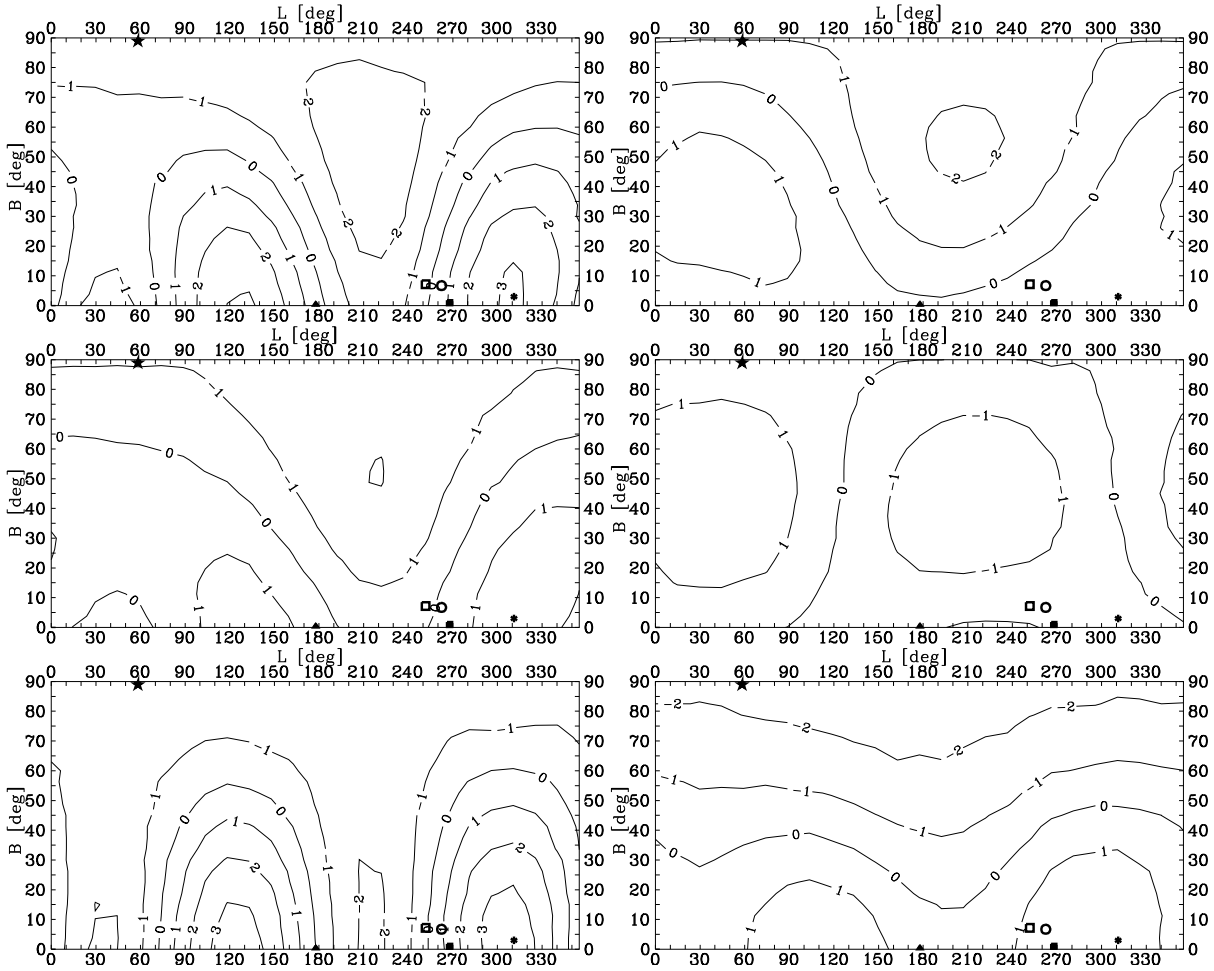


Figure 11. Maps of $s \equiv \Delta_{11}/\sigma(\Delta_{11})$ versus the chosen cluster pole supergalactic co-ordinates (L, B) for the Cluster 12. In the maps, the results of the Tully data are shown on the left, while results obtained with help of HHD and FP corrections are given on the right. The maps are presented for all cluster galaxies (upper panel), as well as for spiral (middle panel) and non-spiral (bottom panel) sub-samples. In the map, we indicate the important directions, as seen from the center of the considered cluster: (1.) three cluster poles (full star, square and triangle), (2.) the direction to the Local Supercluster center (open circle), (3.) the direction of the Virgo A cluster center (open square) and (4.) the line-of-sight from the Earth (asterisk).

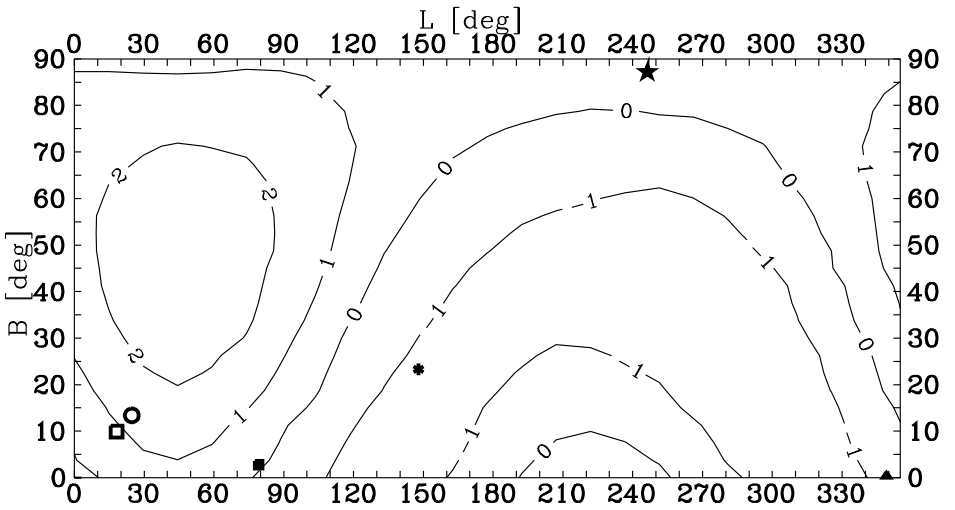


Figure 12. *Cont.*

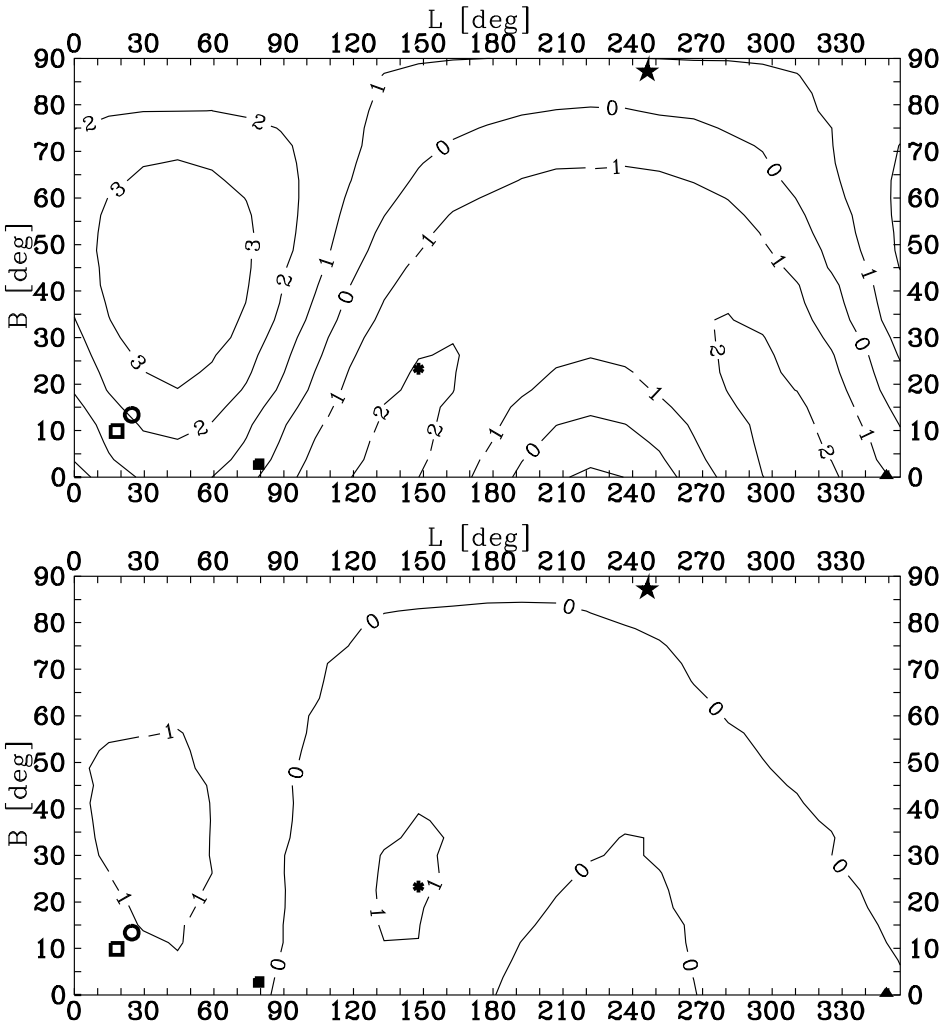


Figure 12. Maps of $s \equiv \Delta_{11}/\sigma(\Delta_{11})$ versus the chosen cluster pole supergalactic co-ordinates (L, B) for the Cluster 15, with results obtained with help of HHD and FP corrections. The maps are presented for all cluster galaxies (upper), as well as for spiral (middle) and non-spiral (bottom) sub-samples. In the map, we indicate the important directions, as seen from the center of the considered cluster: (1.) three cluster poles (full star, square and triangle), (2.) the direction to the Local Supercluster center (open circle), (3.) the direction of the Virgo A cluster center (open square) and (4.) the line of sight from the Earth (asterisk).

5. Conclusions

Data from the Tully Nearby Galaxies Catalog were used to implement a new research method. It also made it possible to check the results of the method using research papers containing a detailed analysis of the orientation of galaxies belonging to the catalog. The obtained results seem to confirm the effectiveness of the new method. However, when calculating, one should also take into account catalog effects specific to the analyzed data. The obtained data show that the omission of the Holmberg effect in the case of data from galaxy catalogs, for which this effect is significant, does not lead to correct results. It should be noted, however, that the current dominant view is that for catalogs based on automatic galaxy measurements, the Holmberg effect should not be significant. In order to fully assess the effectiveness of the new method of investigation of the orientation of galaxies, trials on other observational data are planned.

Additionally, we confirmed that in small groups and clusters of galaxies, such as Tully clusters, there is no galaxy alignment. This is consistent with previous observations,

in which the alignment of galaxies in the structures increases with their mass and is not observed in small groups and clusters of galaxies, in contrast to rich clusters of galaxies, where such ordering is observed. This result is important from the point of view of testing scenarios for the formation of galaxies and their structures. This is because, some models, such as the original hierarchical clustering model [65], do not predict the alignment of galaxies in the structures at all, and other models, such as primordial turbulence [66] or the new version of the Zeldovich pancake model [67], predict the ordering of the orientation of galaxies in clusters, but are unable to explain the dependence of this effect on the mass of the structure. Fortunately, there are also models that predict that the ordering of galaxies in clusters increases with their number [68,69].

However, it should be remembered that the correct scenario for the formation of galaxies and their structures must take into account the existence of dark matter. This is the main problem with most such models, which have difficulty accounting for the existence of dark matter. Only models based on the idea of hierarchical clustering [65], including, in particular, its new version, taking into account tidal effects [68], explicitly takes into account the presence of dark matter, although also in the Li model [69] is the existence of dark matter as a background taken into account.

This means that the observational picture discussed above favors galaxy formation and structure scenarios that predict such a relationship, and takes dark matter into account, as, for example, tidal torque scenarios in the hierarchical clustering model [68], however, the Li model [69] is also allowed. Moreover, our results (lack of alignment in Tully's group) suggest that small-scale, local environmental effects dominate over cosmic anisotropy. Finally, it should be noted that our method is of great importance for the future study of galaxy clusters. Recently, new surveys of galaxies have appeared, such as, for example, SDSS Sky Surveys [70,71], DESI [72] and Euclid [73]. On the basis of these surveys, catalogs of galaxy clusters can be compiled. However, the most important difficulty in studying the orientation of galaxies in these clusters is the problem of determining their morphological types, which has not been satisfactorily solved so far. As we have shown, our method allows such studies in the absence of knowledge of the morphological types of member galaxies. If the shapes of the galaxies are determined correctly and there is no need photometric correction, then our method can be applied directly. However, if this condition is not met, there will be a need to estimate a prior photometric correction, such as FP correction.

Author Contributions: Conceptualization, W.G.; methodology, W.G. and B.M.; software, W.G. and B.M.; validation, W.G. and B.M.; formal analysis, W.G. and B.M.; investigation, W.G. and B.M.; resources, W.G. ; data curation, W.G. and B.M.; writing—original draft preparation, W.G. and B.M.; writing—review and editing, W.G. and B.M.; visualization, B.M.; supervision, W.G. All authors have read and agreed to the published version of the manuscript.

Funding: This research received no external funding.

Institutional Review Board Statement: Not applicable.

Informed Consent Statement: Not applicable.

Data Availability Statement: Detailed data is available from the authors upon request.

Conflicts of Interest: The authors declare no conflict of interest.

Appendix A. Fourier Test

Equation (10), taking into account only the first two modes, can be written in the form:

$$\frac{N_k - N_{0,k}}{N_{0,k}} = \Delta_{11} \cos 2\theta_k + \Delta_{21} \sin 2\theta_k + \Delta_{12} \cos 4\theta_k + \Delta_{22} \sin 4\theta_k. \quad \text{(A1)}$$

whose solution takes the form (details of this type of equations are presented in Chapter 9.2, in [74]):

$$\mathbf{I} = -\left(\mathbf{A}^T\mathbf{G}_y\mathbf{A}\right)^{-1}\mathbf{A}^T\mathbf{G}_y\mathbf{y} \tag{A2}$$

where $\mathbf{A}$ is the matrix of coefficients, in particular Δ_{ij}:

$$\mathbf{A} = \begin{pmatrix} \cos 2\theta_1 & \sin 2\theta_1 & \cos 4\theta_1 & \sin 4\theta_1 \\ \cos 2\theta_2 & \sin 2\theta_2 & \cos 4\theta_2 & \sin 4\theta_2 \\ \vdots & \vdots & \vdots & \vdots \\ \cos 2\theta_k & \sin 2\theta_k & \cos 4\theta_k & \sin 4\theta_k \end{pmatrix} \tag{A3}$$

$\mathbf{y}$ is the vector of particular $y_i = \frac{N_k - N_{0,k}}{N_{0,k}}$:

$$\mathbf{y} = \begin{pmatrix} \frac{N_1 - N_{0,1}}{N_{0,1}} \\ \frac{N_2 - N_{0,2}}{N_{0,2}} \\ \vdots \\ \frac{N_k - N_{0,k}}{N_{0,k}} \end{pmatrix} \tag{A4}$$

$\mathbf{G}_y$ is the inverse matrix to the covariance matrix of particular y_i i.e., weight matrix:

$$\mathbf{G}_y = \begin{pmatrix} N_{0,1} & 0 & \cdots & 0 \\ 0 & N_{0,2} & 0 & \vdots \\ \vdots & 0 & \ddots & 0 \\ 0 & \cdots & 0 & N_{0,k} \end{pmatrix} \tag{A5}$$

and the inverted covariance matrix takes the form $\mathbf{G} = \mathbf{A}^T\mathbf{G}_y\mathbf{A}$. Using the auxiliary vector $\mathbf{H} = \mathbf{A}^T\mathbf{G}_y\mathbf{y}$, Equation (A2) can be written as:

$$\mathbf{I} = \mathbf{G}^{-1} \cdot \mathbf{H} \tag{A6}$$

Using the notations:

$$\begin{aligned} A &= \sum_{k=1}^{n} N_{0,k}\cos^2 2\theta_k, B = \sum_{k=1}^{n} N_{0,k}\sin^2 2\theta_k, \\ C &= \sum_{k=1}^{n} N_{0,k}\cos^2 4\theta_k, D = \sum_{k=1}^{n} N_{0,k}\sin^2 4\theta_k, \\ U &= \sum_{k=1}^{n} N_{0,k}\cos 2\theta_k \cos 4\theta_k, W = \sum_{k=1}^{n} N_{0,k}\sin 2\theta_k \sin 4\theta_k, \\ Y &= \sum_{k=1}^{n} N_{0,k}\cos 2\theta_k \sin 2\theta_k, X = \sum_{k=1}^{n} N_{0,k}\sin 2\theta_k \cos 4\theta_k, \\ Z &= \sum_{k=1}^{n} N_{0,k}\cos 4\theta_k \sin 4\theta_k, V = \sum_{k=1}^{n} N_{0,k}\cos 2\theta_k \sin 4\theta_k, \\ K &= \sum_{k=1}^{n} (N_k - N_{0,k})\cos 2\theta_k, L = \sum_{k=1}^{n} (N_k - N_{0,k})\sin 2\theta_k, \\ M &= \sum_{k=1}^{n} (N_k - N_{0,k})\cos 4\theta_k, N = \sum_{k=1}^{n} (N_k - N_{0,k})\sin 4\theta_k, \end{aligned} \tag{A7}$$

the expressions for matrix **G** and vector **H** will take the form:

$$\mathbf{G} = \begin{pmatrix} A & Y & U & V \\ Y & B & X & W \\ U & X & C & Z \\ V & W & Z & D \end{pmatrix} \tag{A8}$$

and

$$\mathbf{H} = \begin{pmatrix} K \\ L \\ M \\ N \end{pmatrix}. \tag{A9}$$

As a consequence, the Δ_{ij} coefficients of the vector I described by Equation (21) will be expressed by:

$$\begin{aligned} \Delta_{11} &= \frac{S_1K + S_5M + S_7L + S_8N}{R} \\ \Delta_{21} &= \frac{S_2L + S_6N + S_7K + S_9M}{R} \\ \Delta_{12} &= \frac{S_3M + S_5K + S_9L + S_{10}N}{R} \\ \Delta_{22} &= \frac{S_4N + S_6L + S_8K + S_{10}M}{R} \end{aligned} \tag{A10}$$

where

$$\begin{aligned} S_1 &= C(BD - W^2) + X(2WZ - DX) - Z^2B \\ S_2 &= D(AC - U^2) + V(2UZ - CV) - Z^2A \\ S_3 &= A(BD - W^2) + Y(2WV - DY) - V^2B \\ S_4 &= B(AC - U^2) + Y(2UX - CY) - X^2A \\ S_5 &= -U(BD - W^2) + Y(DX - WZ) + V(BZ - WX) \\ S_6 &= -W(AC - U^2) + Z(AX - UY) + V(CY - UX) \\ S_7 &= V(CW - XZ) + Y(Z^2 - CD) + U(DX - WZ) \\ S_8 &= Y(CW - XZ) + V(X^2 - BC) + U(BZ - WX) \\ S_9 &= Z(AW - VY) + X(V^2 - AD) + U(DY - VW) \\ S_{10} &= X(AW - VY) + Z(Y^2 - AB) + U(BV - WY) \\ R &= (AC - U^2)(BD - W^2) + Y(2W(CV - UZ) + 2X(DU - ZV) + \\ &+ Y(Z^2 - CD)) + V(2U(BZ - XW) - BCV) + X^2(V^2 - AD) + ZA(2XW - ZB) \end{aligned} \tag{A11}$$

The variable J appearing in the Formula (20) will be expressed by the relation:

$$\begin{aligned} J = {} & A\Delta_{11}^2 + B\Delta_{21}^2 + C\Delta_{12}^2 + D\Delta_{22}^2 + 2Y\Delta_{11}\Delta_{21} + 2U\Delta_{11}\Delta_{12} + \\ & + 2V\Delta_{11}\Delta_{22} + 2X\Delta_{21}\Delta_{12} + 2W\Delta_{21}\Delta_{22} + 2Z\Delta_{12}\Delta_{22} \end{aligned} \tag{A12}$$

For the case of a symmetric theoretical distribution, i.e., when $N_{0i} = N_{0n-i}$, the values of the coefficients X, Y, V, Z are equal to 0 [9] and, consequently, Formulas (A10) are simplified to the form

$$\begin{aligned} \Delta_{11} &= \frac{CK - UM}{AC - U^2} \\ \Delta_{21} &= \frac{DL - WN}{BD - W^2} \\ \Delta_{12} &= \frac{AM - UK}{AC - U^2} \\ \Delta_{22} &= \frac{BN - WL}{BD - W^2} \end{aligned} \tag{A13}$$

which is similar to the formula for the variable J, reduced to the form

$$J = A\Delta_{11}^2 + B\Delta_{21}^2 + C\Delta_{12}^2 + D\Delta_{22}^2 + 2U\Delta_{11}\Delta_{12} + 2W\Delta_{21}\Delta_{22} \tag{A14}$$

It should be noted that the applicability limits of Formulas (A13) may be extended in cases for which the Formulas (A10) should be applied, if it is possible to indicate a relatively small asymmetry of theoretical distributions.

When only the first modes are taken into account in the Fourier test, i.e., when vector **I** is given by relation (18), then vector **A** takes the form

$$\mathbf{A} = \begin{pmatrix} \cos 2\theta_1 & \sin 2\theta_1 \\ \cos 2\theta_2 & \sin 2\theta_2 \\ \vdots & \vdots \\ \cos 2\theta_k & \sin 2\theta_k \end{pmatrix} \tag{A15}$$

following this, matrix **G** and vector **H** are given by:

$$\mathbf{G} = \begin{pmatrix} A & Y \\ Y & B \end{pmatrix} \tag{A16}$$

and

$$\mathbf{H} = \begin{pmatrix} K \\ L \end{pmatrix} \tag{A17}$$

In the most general form, Δ_{1j} coefficients are then expressed by formulas

$$\begin{aligned} \Delta_{11} &= \frac{BK - YL}{AB - Y^2} \\ \Delta_{21} &= \frac{AL - YK}{AB - Y^2} \end{aligned} \tag{A18}$$

Additionally, the variable J in the Formula (17) has the form

$$J = A\Delta_{11}^2 + B\Delta_{21}^2 + 2Y\Delta_{11}\Delta_{21} \tag{A19}$$

In the case of a symmetric theoretical distribution, Y is equal to 0, so these formulas are simplified to (11), (12) and (16).

Appendix B. Influence of Division into Bins on the Values of the Obtained Statistical Tests

The values of the obtained statistical tests depend on the method of dividing the range of the analyzed angles into bins. In the works dealing with the study of the orientation of galaxies in clusters [9,48,49], approaches were used to perform analyses using a different number of intervals, and comparing the obtained differences. This is the recommended way

of proceeding, among others, in cases where the number of analyzed galaxies is small and does not satisfy theoretical test conditions, as well as in the case of tests that are particularly sensitive to the binning procedure, such as the Kolmogorov tests.

Alternatively, for some statistical tests, it is also possible to repeat the analysis without dividing the angle ranges into bins. The Kolmogorov–Smirnov test, Cramer von-Mises test and Watson test, calculated in this way, are presented in Tables A1–A4. These tables also contain the results of these tests calculated using divisions into 18 bins. Analysis of the Kolmogorov—Smirnov and Cramer von-Mises tests showed that, in the case of our research, with calculations using both methods, the obtained statistical values do not differ significantly. An analogous situation also takes place in the case of variable $\bar{F}$ in Formula (25), but for the range of the angle divided into bins, the values of the variable are "shifted" in the direction of "larger values". This tendency is reflected in the values of the U^2 statistic. Here, however, the deviations are larger and in both directions, which means that in a certain number of cases, we get negative values in terms of the U^2 statistic. CDF values for Kolmogorov, Cramer-von Mises and Watson tests are presented in Figure A1. This proves that, at least for the Watson test, the binning process is important. As a result, if we compare the statistics obtained for the actual distributions of the orientation angles of the galaxies with the theoretical distributions of galaxies, we must remember that the binning process is the same in both cases (and this is what we do in present paper).

Table A1. Comparison of statistical tests calculated by dividing and not dividing the range of the analyzed angle δ_D into bins, with the inclination taken directly from the NBG Catalog.

Group	Angle Range Not Divided into Bins				Angle Range Divided into 18 Bins			
	λ	W^2	$\bar{F}$	U^2	λ	W^2	$\bar{F}$	U^2
11	1.332	0.6221	0.5021	0.6193	1.197	0.6769	0.5367	−0.1641
12	0.792	0.1445	0.5041	0.1388	0.549	0.1183	0.5374	−0.3470
13	0.645	0.0515	0.5023	0.0509	0.621	0.0726	0.5357	−0.0905
14	0.852	0.2021	0.5123	0.1376	0.779	0.1772	0.5493	−0.8586
15	0.619	0.0478	0.4889	0.0318	0.589	0.0612	0.5223	−0.0036
17	0.882	0.1242	0.4680	0.0421	0.818	0.1604	0.5002	0.1604
21	1.280	0.4832	0.4610	0.1051	1.143	0.4859	0.4947	0.4789
22	0.849	0.1455	0.5278	0.0481	0.618	0.1290	0.5568	−0.2775
23	0.657	0.0624	0.4944	0.0592	0.468	0.0670	0.5286	−0.0148
31	1.982	1.3491	0.4321	0.3796	1.794	1.3340	0.4656	1.0848
41	1.473	0.5381	0.5365	0.2828	1.371	0.5135	0.5710	−0.4546
42	0.915	0.2320	0.5265	0.0705	0.747	0.2420	0.5604	−0.5970
44	1.273	0.4698	0.5518	0.2551	1.336	0.4800	0.5885	−0.1473
51	1.508	0.5760	0.4644	0.2862	1.443	0.5956	0.4990	0.5954
52	1.528	0.6346	0.4547	0.2816	1.417	0.6913	0.4897	0.6731
53	0.723	0.1024	0.4888	0.0698	0.620	0.0862	0.5241	−0.0647
61	0.728	0.0932	0.4993	0.0930	0.615	0.0900	0.5320	−0.1735
64	1.007	0.2512	0.5375	0.1075	0.836	0.2517	0.5696	−0.2426

Table A2. Comparison of statistical tests calculated by dividing and not dividing the range of the analyzed angle η into bins, with he inclination taken directly from the NBG Catalog.

Group	Angle Range Not Divided into Bins				Angle Range Divided into 18 Bins			
	λ	W^2	$\bar{F}$	U^2	λ	W^2	$\bar{F}$	U^2
11	2.089	1.2378	0.4744	0.8272	2.003	1.2774	0.5020	1.2750
12	1.810	1.0361	0.5449	0.3667	1.756	0.9940	0.5723	−0.7409
13	0.914	0.1862	0.5132	0.1638	0.766	0.2142	0.5430	−0.0221
14	1.142	0.3100	0.5177	0.1769	1.001	0.2964	0.5455	−0.5861
15	1.020	0.2726	0.4606	0.0707	0.906	0.2649	0.4910	0.2545
17	0.548	0.0570	0.4946	0.0546	0.460	0.0467	0.5236	0.0021
21	1.274	0.3330	0.5241	0.1894	1.228	0.2912	0.5515	−0.3671
22	1.004	0.1719	0.4771	0.1058	0.980	0.1935	0.5040	0.1915
23	1.163	0.3179	0.4610	0.1660	1.089	0.2968	0.4900	0.2868
31	1.744	0.6451	0.4533	0.1865	1.564	0.6733	0.4820	0.6054
41	1.967	0.8206	0.4525	0.3880	1.949	0.8840	0.4800	0.8075
42	1.231	0.5851	0.5403	0.2119	1.238	0.5716	0.5679	−0.4880
44	0.731	0.1182	0.5119	0.1068	0.783	0.1229	0.5424	−0.0206
51	1.187	0.3431	0.4732	0.1790	1.148	0.3636	0.5012	0.3633
52	1.927	1.0018	0.4408	0.3992	1.923	1.1189	0.4671	0.9322
53	0.434	0.0278	0.4999	0.0278	0.338	0.0229	0.5286	−0.1903
61	0.775	0.0735	0.4956	0.0685	0.643	0.0716	0.5243	−0.0812
64	2.056	1.1930	0.4116	0.3966	1.881	1.4348	0.4368	1.0276

Table A3. Comparison of statistical tests calculated by dividing and not dividing the range of the analyzed angle δ_D into bins, with the inclination obtained by taking into account the morphological types of galaxies and the Fouque and Paturel correction.

Group	Angle Range Not Divided into Bins				Angle Range Divided into 18 Bins			
	λ	W^2	$\bar{F}$	U^2	λ	W^2	$\bar{F}$	U^2
11	0.713	0.0803	0.4983	0.0784	0.677	0.0710	0.5325	−0.5891
12	0.593	0.0551	0.4997	0.0550	0.384	0.0455	0.5351	−0.3625
13	0.830	0.1985	0.5056	0.1945	0.786	0.2241	0.5389	0.0307
14	0.731	0.0988	0.5089	0.0651	0.623	0.1024	0.5444	−0.7387
15	0.771	0.0949	0.5131	0.0726	0.789	0.0932	0.5482	−0.2091
17	0.622	0.1100	0.4664	0.0197	0.559	0.0890	0.4999	0.0890
21	0.928	0.1562	0.4786	0.0421	0.889	0.1671	0.5118	0.1328
22	0.938	0.1272	0.5157	0.0962	0.707	0.1110	0.5488	−0.1888
23	0.762	0.1337	0.5162	0.1074	0.614	0.1435	0.5487	−0.0934
31	1.140	0.2597	0.4738	0.1159	0.966	0.2677	0.5075	0.2560
41	0.834	0.2486	0.5301	0.0751	0.722	0.2679	0.5628	−0.4889
42	0.992	0.2092	0.5212	0.1054	0.786	0.1954	0.5525	−0.4389
44	1.004	0.2639	0.5419	0.1233	0.900	0.2598	0.5777	−0.2228
51	0.638	0.0958	0.4838	0.0362	0.552	0.0833	0.5185	0.0054
52	1.580	0.7954	0.4434	0.2440	1.454	0.7803	0.4799	0.7109
53	0.621	0.0842	0.5130	0.0401	0.523	0.0901	0.5479	−0.5060
61	0.989	0.1736	0.4810	0.0804	0.802	0.1902	0.5125	0.1498
64	0.686	0.0856	0.5184	0.0510	0.594	0.0868	0.5513	−0.1816

Table A4. Comparison of statistical tests calculated by dividing and not dividing the range of the analyzed angle η into bins, with the inclination obtained by taking into account the morphological types of galaxies and the Fouque and Paturel correction.

Group	Angle Range Not Divided into Bins				Angle Range Divided into 18 Bins			
	λ	W^2	$\bar{F}$	U^2	λ	W^2	$\bar{F}$	U^2
11	1.182	0.4085	0.4981	0.4062	1.101	0.4450	0.5249	0.0557
12	1.015	0.2816	0.5238	0.0936	0.860	0.2365	0.5490	−0.5615
13	1.303	0.2504	0.4681	0.1204	1.110	0.2416	0.4970	0.2405
14	0.939	0.1626	0.5122	0.0997	0.775	0.1649	0.5406	−0.5359
15	0.841	0.2022	0.4684	0.0725	0.643	0.1576	0.4991	0.1575
17	0.824	0.1234	0.4678	0.0403	0.683	0.1061	0.4965	0.1052
21	0.678	0.0876	0.4859	0.0381	0.564	0.0917	0.5139	0.0438
22	0.452	0.0394	0.4997	0.0394	0.535	0.0286	0.5273	−0.0656
23	0.537	0.0514	0.5009	0.0513	0.444	0.0477	0.5278	−0.0294
31	1.292	0.2844	0.4694	0.0877	1.104	0.3029	0.4966	0.3005
41	1.209	0.2698	0.4883	0.2434	0.962	0.2555	0.5174	0.1976
42	0.900	0.2695	0.5276	0.0943	0.879	0.2468	0.5543	−0.4326
44	0.592	0.0703	0.4838	0.0492	0.472	0.0678	0.5139	0.0524
51	1.423	0.3883	0.4668	0.1367	1.214	0.4058	0.4946	0.3993
52	1.362	0.5905	0.4536	0.2205	1.339	0.6194	0.4793	0.5459
53	0.788	0.0917	0.4900	0.0657	0.675	0.0943	0.5167	0.0221
61	1.087	0.2415	0.4748	0.0781	0.955	0.2249	0.5039	0.2211
64	0.779	0.1157	0.4940	0.1120	0.627	0.1198	0.5218	0.0714

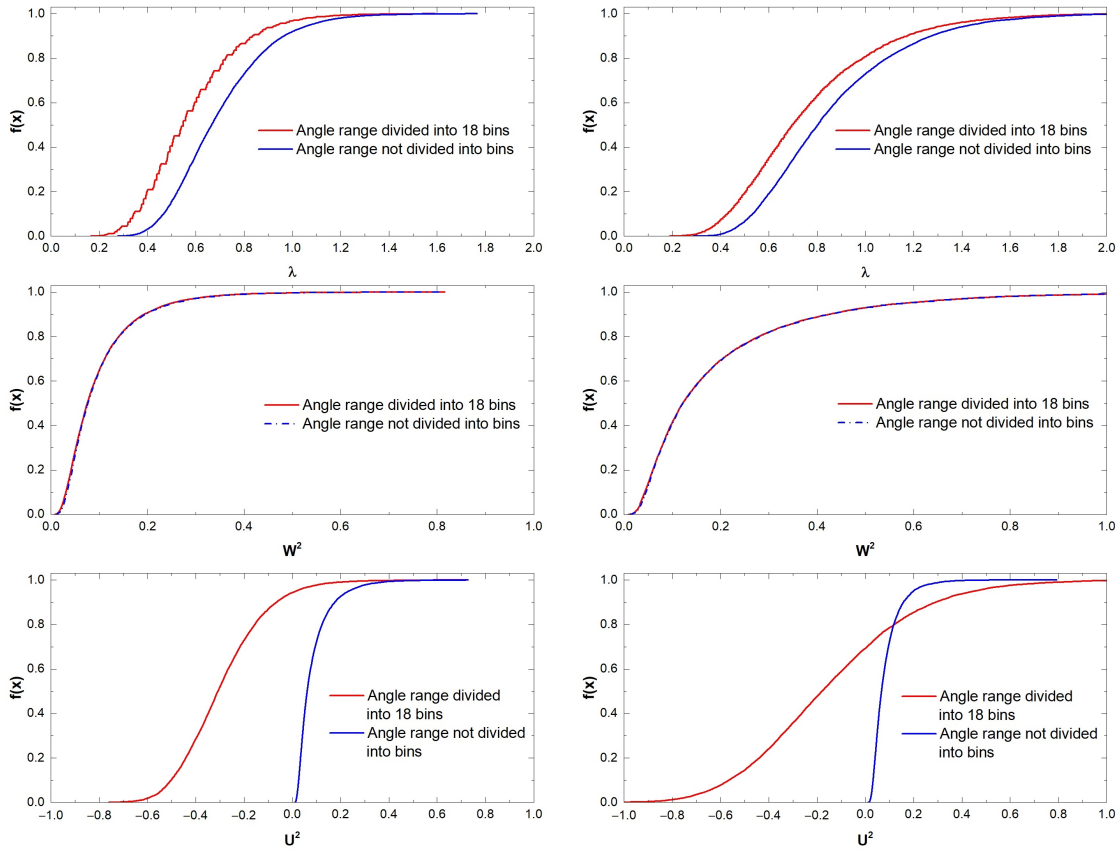


Figure A1. The Cumulative Distribution Function (CDF) of the angle δ_D (left panel) and η (right panel) for analyzed statistics for group 12. Comparison of statistical tests calculated by dividing and not dividing the range of the analyzed angles into bins From up to down, we present statistics: λ, W^2 and U^2.

References

1. Romanowsky, A.J.; Fall, S.M. Angular Momentum and Galaxy Formation Revisited. *Astrophys. J. Suppl.* **2015**, *203*, 17. [CrossRef]
2. Joachimi, B.; Cacciato, M.; Kitching, T.D.; Leonard, A.; Mandelbaum, R.; Schäfer, B.M.; Sifón, C.; Hoekstra, H.; Kiessling, A.; Kirk, D. Rassat A Galaxy Alignments: An Overview. *Space Sci. Rev.* **2015**, *193*, 1. [CrossRef]
3. Kiessling, A.; Cacciato, M.; Joachimi, B.; Kirk, D.; Kitching, T.D.; Leonard, A.; Mandelbaum, R.; Schäfer, B.M.; Sifón, C.; Brown, M.L.; et al. Galaxy Alignments: Theory, Modelling & Simulations. *Space Sci. Rev.* **2015**, *193*, 67.
4. Peebles, P.J.E.; Yu, J.T. Primeval Adiabatic Perturbation in an Expanding Universe. *Astrophys. J.* **1970**, *162*, 815. [CrossRef]
5. Silk, J. Cosmic Black-Body Radiation and Galaxy Formation. *Astrophys. J.* **1968**, *151*, 459. [CrossRef]
6. Sunyaev, R.A.; Zeldovich, Y.B. Small-Scale Fluctuations of Relic Radiation. *Astrophys. Space Sci.* **1970**, *7*, 3–19. [CrossRef]
7. Stephanovich, V.A.; Godłowski, W. The Distribution of Galaxies' Gravitational Field Stemming from Their Tidal Interaction. *Astrophys. J.* **2015**, *810*, 14. [CrossRef]
8. Godłowski, W.; Flin, P. The Orientations of Galaxy Groups and Formation of the Local Supercluster. *Astrophys. J.* **2010**, *708*, 920. [CrossRef]
9. Pajowska, P.; Godłowski, W.; Zhu, Z.-H.; Popiela, J.; Panko, E.; Flin, P. Investigation of the orientation of galaxies in clusters: The importance, methods and results of research. *J. Cosmol. Astropart. Phys.* **2019**, *2*, 5. [CrossRef]
10. Wang, P.; Libeskind, N.I.; Tempel, E.; Pawlowski, M.S.; Kang, X.; Guo, Q. The Alignment of Satellite Systems with Cosmic Filaments in the SDSS DR12. *Astrophys. J.* **2020**, *900*, 8. [CrossRef]
11. Moon, J.S.; An S.H.; Yoon, S.J. Living with Neighbors. III. The Origin of the Spin-Orbit Alignment of Galaxy Pairs: A Neighbor versus the Large-scale Structure. *Astrophys. J.* **2021**, *909*, 15. [CrossRef]
12. Tovmassian, H.M. On the Problem of the Galaxy Alignment with Groups and Clusters. *Astrophysics* **2021**, *64*, 141. [CrossRef]
13. Yuan, Z.S.; Wen, Z.L. The alignment between brightest cluster galaxies and host clusters. *Mon. Not. R. Astron. Soc.* **2022**, *516*, 3159. [CrossRef]
14. Petit, Q.; Ducourant, C.; Slezak, E.; Sluse, D.; Delchambre, L. Shape, alignment, and mass distribution of baryonic and dark-matter halos in one EAGLE simulation. *Astron. Astrophys.* **2023**, *669*, 18. [CrossRef]
15. Trujillo, I.; Carretero, C.; Patri, G. Detection of the effect of cosmological large-scale structure on the orientation of galaxies. *Astrophys. J.* **2006**, *640*, L111. [CrossRef]
16. Varela, J.; Betancort-Rijo, J.; Trujillo, I.; Ricciardelli, E. The orientation of disk galaxies around large cosmic voids. *Astrophys. J.* **2012**, *744*, 82. [CrossRef]
17. Okabe, T.; Nishimichi, T.; Oguri, M.; Peirani, S.; Kitayama, T.; Sasaki, S.; Suto, Y. Projected alignment of non-sphericities of stellar, gas and dark matter distributions in galaxy clusters: Analysis of the Horizon-AGN simulation. *Mon. Not. R. Astron. Soc.* **2018**, *478*, 1141. [CrossRef]
18. Codis, S.; Jindal, A.; Chisari, N.E.; Vibert, D.; Dubois, Y.; Pichon, C.; Devriendt, J. Galaxy orientation with the cosmic web across cosmic time. *Mon. Not. R. Astron. Soc.* **2018**, *481*, 4753. [CrossRef]
19. Ciotti, L.; Dutta, S.N. Alignment and morphology of elliptical galaxies: The influence of thecluster tidal field. *Mon. Not. R. Astr. Soc.* **1994**, *270*, 390. [CrossRef]
20. Ciotti, L.; Giampieri, G. Motion of a Rigid Body in a Tidal Field: An application to elliptical galaxies in clusters. *Cel. Mec.* **1997**, *68*, 313. [CrossRef]
21. Thompson, L.A. The Angular Momentum Properties of Galaxies in Rich Clusters. *Astron. J.* **1976**, *209*, 22–34. [CrossRef]
22. Godłowski, W.; Piwowarska, P.; Panko, E.; Flin, P. The Orientation of Galaxies in Galaxy Clusters. *Astrophys. J.* **2010**, *723*, 985–992. [CrossRef]
23. Hutsemekers, D. Evidence for Very Large-Scale Coherent Orientations of Quasar Polarization Vectors. *Astron. Astrophys.* **1998**, *332*, 410.
24. Hutsemekers, D.; Cabanac, R.; Lamy, H.; Sluse, D. Mapping extreme-scale alignments of Quasar Polarization Vectors. *Astron. Astrophys.* **2005**, *441*, 915. [CrossRef]
25. Migkas, K.; Pacaud, F.; Schellenberger, G.; Erler, J.; Nguyen-Dang, N.T.; Reiprich, T.H.; Ramos-Ceja, M.E.; Lovisari, L. Cosmological implications of the anisotropy of ten galaxy cluster scaling relations. *Astron. Astrophys.* **2021**, *649*, 115. [CrossRef]
26. Hawley, D.L.; Peebles, P.J.E. Distribution of observed orientations of galaxies. *Astron. J.* **1975**, *80*, 477–491. [CrossRef]
27. Godłowski, W. Remarks on the Methods of Investigations of Alignment of Galaxies. *Astrophys. J.* **2012**, *747*, 7. [CrossRef]
28. Öpik, E.J. Preferential Orientation of Galaxies: On the Possibility of Detection. *Ir. Astron. J.* **1970**, *9*, 211.
29. Jaaniste, J. The accretion spiral. *Tartu Obs.* **1977**, 50–67.
30. Jaaniste, J.; Saar, E. Orientation of Spiral Galaxies as a Test of Theories of Galaxy Formation. In *The Large Scale Structures of the Universe, Proceedings of the Symposium, Tallin, Estonian, 12–16 September 1977*; Longair, M.S., Einasto, J., Eds.; IAU Symposium, No. 79; D. Reidel Publishing Co.: Dordrecht, The Netherlands, 1978; p. 488.
31. Flin, P.; Godłowski, W. The orientation of galaxies in the Local Supercluster. *Mon. Not. R. Astr. Soc.* **1986**, *222*, 525–541. [CrossRef]
32. Holmberg, E. On the Apparent Diameters and the Orientation in Space of Extragalactic Nebulae. *Medd. Fran Lunds Astron. Obs. Ser. II* **1946**, *117*, 3–82.
33. Holmberg, E. On the A photographic photometry of extragalactic nebulae. *Medd. Lund. Astron. Obs. Ser. II* **1958**, *136*, 1.
34. Holmberg, E. Magnitudes, Colors, Surface Brightness, Intensity Distributions Absolute Luminosities, and Diameters of Galaxies. In *Galaxies and the Universe*; Sandage, A., Sandage, M., Kristian, J., Eds.; University of Chicago Press: Chicago, IL, USA, 1975; p. 123.

35. Fouque, P.; Paturel, G. Standard photometric diameters of galaxies. II. Reduction of the ESO,UGC, MCG catalogues. *Astron. Astroph.* **1985**, *150*, 192–204.
36. Tully, R.B. *Nearby Galaxies Catalogue (NBG)*, 2nd ed.; Cambridge University Press: Cambridge, UK, 1988. Available online: https://vizier.cds.unistra.fr/viz-bin/VizieR?-source=VII/145 (accessed on 7 April 2023).
37. Dressler, A. A catalog of morphological types in 55 rich clusters of galaxies. *Astrophys. J. Suppl. Ser.* **1980**, *42*, 565–609. [CrossRef]
38. Calvi, R.; Poggianti, B.M.; Fasano, G.; Vulcani, B. The distribution of galaxy morphological types and the morphology-mass relation in different environments at low redshift. *Mon. Not. R. Astr. Soc.* **2012**, *419*, L14–L18. [CrossRef]
39. Coenda, V.; Muriel, H.; Martinez, H.J. Comparing galaxy populations in compact and loose groups of galaxies. *Astron. Astrophys.* **2012**, *543*, 12. [CrossRef]
40. Hoyle, B.; Masters, K.L.; Nichol, R.C.; Jimenez, R.; Bamford, S.P. The fraction of early-type galaxies in low-redshift groups and clusters of galaxies. *Mon. Not. R. Astr. Soc.* **2012**, *423*, 3478–3485. [CrossRef]
41. Tully, R.B. Nearby Groups of Galaxies. II. an All-Sky Survey within 3000 Kilometers per Second. *Astrophys. J.* **1987**, *321*, 280. [CrossRef]
42. Lauberts, A. *ESO/Uppsala Survey of the ESO B Atlas*, 1st ed.; European Southern Observatory: Garching, Germany, 1982.
43. Lauberts, A.; Valentijn, E. *The Surface Photometry Catalogue of the ESO-Uppsala Galaxies*, 1st ed.; European Southern Observatory: Garching, Germany, 1989.
44. Nilson, P. *Uppsala General Catalogue of Galaxies*; Uppsala Astronomiska Observatoriums Annaler; Astronomiska Observatorium: Uppsala, Sweden, 1973; Volume 1.
45. Nilson, P. *Catalogue of Selected Non-UGC Galaxies*; Uppsala Astronomical Observatory Reports 5; Astronomiska Observatorium: Uppsala, Sweden, 1974.
46. Tully, R.B.; Shaya, E.J. Infall of galaxies into the virgo cluster and some cosmological constraints. *Astrophys. J.* **1984** *281*, 31. [CrossRef]
47. Godłowski, W.; Ostrowski, M. Investigation of galactic alignment in Local Supercluster galaxy clusters. *Mon. Not. R. Astr. Soc.* **1999**, *303*, 50–64. [CrossRef]
48. Godłowski, W. Some observational aspects of the orientation of galaxies. *Acta Phys. Pol. B* **2011**, *42*, 2323–2334. [CrossRef]
49. Pajowska, P.; Godlowski, W.; Panko, E.; Flin, P. Some aspects of the orientation of galaxies in clusters. *J. Phys. Stud.* **2012**, *16*, 4901. [CrossRef]
50. Aryal, B.; Kafle, P.R.; Saurer, W. Radial velocity dependence in the spatial orientations of galaxies in and around the local supercluster. *Mon. Not. R. Astr. Soc.* **2006**, *389*, 471. [CrossRef]
51. Feigelson, E.D.; Babu, G.J. *Modern Statistical Methods for Astronomy with R Applications*; Cambridge University Press: Cambridge, UK, 2012.
52. von Mises, R. *Wahrscheinlichkeit Statistic Und Wahrheit*, 1st ed.; Verlag von Julius Springer: Vienna, Austria, 1928.
53. Cramér, H. On the composition of elementary errors. *Scand. Actuar. J.* **1928**, *1928*, 13–74. [CrossRef]
54. Watson, G.S. Goodness-of-Fit Tests on a Circle. *Biometrika* **1961**, *48*, 109–114. [CrossRef]
55. Watson, G.S. Goodness-of-Fit Tests on a Circle. II. *Biometrika* **1962**, *49*, 57–63. [CrossRef]
56. Heidmann, J.; Heidmann, N.; de Vaucouleurs, G. Inclination and absorption effects on the apparent diameters, optical luminosities and neutral hydrogen radiation of galaxies. *Mem. R. Astron. Soc.* **1972**, *75*, 85.
57. Chernoff, H.; Lehmann, E.L. The Use of Maximum Likelihood Estimates in χ^2 Tests for Goodness of Fit. *Ann. Math. Statist.* **1954**, *25*, 579. [CrossRef]
58. Snedecor, G.W.; Cochran, W.G. *Statistical Methods*; Iowa Univ. Press: Iowa City, IA, USA, 1967.
59. Krysicki, W.; Bartos, J.; Dyczka, W.; Królikowska, K.; Wasilewski, M. *The Probability Calculus and Mathematical Statistics in Exercises (in Polish Rachunek Prawdopodobieństwa i Statystyka Matematyczna w Zadaniach II)*; Warszawa PWN: Warsaw, Poland , 1998.
60. Percival, B.D.; Walden, A.T. *Spectral Analysis for Physical Applications*; Cambridge University Press: Cambridge, UK, 1993.
61. Yu, J.T.; Peebles, P.J.E. Superclusters of Galaxies? *Astrophys. J.* **1969**, *158*, 103. [CrossRef]
62. Newman, W.I., Haynes, M.P., Terzian, Y., Redshift Data and Statistical Inference. *Astrophys. J.* **1994**, *431*, 147. [CrossRef]
63. Godłowski, W.; Bajan, K.; Flin, P. Weak redshift discretisation in the Local Group of galaxies? *Astron. Nachrichten* **2006**, *327*, 103. [CrossRef]
64. Smirnow, N. Table for Estimating the Goodness of Fit of Empirical Distributions. *Ann. Math. Stat.* **1948**, *19*, 279–281. [CrossRef]
65. Peebles, P.J.E. Origin of the Angular Momentum of Galaxies. *Astrophys. J.* **1969**, *155*, 393. [CrossRef]
66. Efstathiou, G.A.; Silk, J. The Formation of Galaxies. *Fundam. Cosm. Phys.* **1983**, *9*, 1. [CrossRef]
67. Shandarin, S.F.; Habib, S.; Heitmann, K. Cosmic web, multistream flows, and tessellations. *Phys. Rev. D* **2012**, *85*, 083005. [CrossRef]
68. Catelan, P.; Theuns, T. Evolution of the angular momentum of protogalaxies from tidal torques: Zel'dovich approximation. *Mon. Not. R. Astr. Soc.* **1996**, *282*, 436.
69. Li, L.X. Effect of the global rotation of the universe on the formation of galaxies. *Gen. Rel. Grav.* **1998**, *30*, 497. [CrossRef]
70. Banerjee, P.; Szabo, T.; Pierpaoli, E.; Franco, G.; Ortiz, M.; Oramas, A.; Tornello, B. An optical catalog of galaxy clusters obtained from an adaptive matched filter finder applied to SDSS DR9 data. *New Astron.* **2018**, *58*, 61. [CrossRef]
71. Wen, Z.L.; Han, J.L. Calibration of the Optical Mass Proxy for Clusters of Galaxies and an Update of the WHL12 Cluster Catalog. *Astrophys. J.* **2015**, *807*, 178. [CrossRef]

72. Zou, H.; Gao, J.; Xu, X.; Zhou, X.; Ma, J.; Zhou, Z.; Zhang, T.; Nie, J.; Wang, J.; Xue, S. Galaxy Clusters from the DESI Legacy Imaging Surveys. I. Cluster Detection. *Astrophys. J. Suppl. Ser.* **2021**, *253*, 56. [CrossRef]
73. Bisigello, L.; Conselice, C.J.; Baes, M.; Bolzonella, M.; Brescia, M.; Cavuoti, S.; Cucciati, O.; Humphrey, A.; Hunt, L.K.; Maraston, C. Euclid preparation—XXIII. Derivation of galaxy physical properties with deep machine learning using mock fluxes and H-band images. *Mon. Not. R. Astr. Soc.* **2023**, *520*, 3529–3548. [CrossRef]
74. Brandt, S. *Data Analysis: Statistical and Computational Methods for Scientists and Engineers*, 4th ed.; Springer: Cham, Switzerland, 2014. [CrossRef]

Disclaimer/Publisher's Note: The statements, opinions and data contained in all publications are solely those of the individual author(s) and contributor(s) and not of MDPI and/or the editor(s). MDPI and/or the editor(s) disclaim responsibility for any injury to people or property resulting from any ideas, methods, instructions or products referred to in the content.